REPORT DOCUMENTATION PAGE

Form Approved OMB NO. 0704-0188

1. REPORT DATE (DD-MM-YYYY)	2. REPORT TYPE	3. DATES COVERED (From - To)
03-08-2014	MS Thesis	-

4. TITLE AND SUBTITLE
Turbulent Flame Stabilization Methods UsingConfinement, Diluents, and High-Potential Electric Fields.

5a. CONTRACT NUMBER
W911NF-12-1-0140

5b. GRANT NUMBER

5c. PROGRAM ELEMENT NUMBER
611102

6. AUTHORS
Andrew Hutchins

5d. PROJECT NUMBER

5e. TASK NUMBER

5f. WORK UNIT NUMBER

7. PERFORMING ORGANIZATION NAMES AND ADDRESSES
North Carolina State University
2701 Sullivan Drive
Suite 240, Campus Bx 7514
Raleigh, NC 27695 -7003

8. PERFORMING ORGANIZATION REPORT NUMBER

9. SPONSORING/MONITORING AGENCY NAME(S) AND ADDRESS (ES)
U.S. Army Research Office
P.O. Box 12211
Research Triangle Park, NC 27709-2211

10. SPONSOR/MONITOR'S ACRONYM(S)
ARO

11. SPONSOR/MONITOR'S REPORT NUMBER(S)
61381-EG.10

12. DISTRIBUTION AVAILIBILITY STATEMENT
Approved for public release; distribution is unlimited.

13. SUPPLEMENTARY NOTES
The views, opinions and/or findings contained in this report are those of the author(s) and should not contrued as an official Department of the Army position, policy or decision, unless so designated by other documentation.

14. ABSTRACT
Presented are three methods in controlling flame stability and enhancing flame control. The three methods that were observed were flame confinement, flame dilution with inert diluents, and high-potential electric field effects on flames. Flames that were under full confinement experienced similar liftoff trends to that of the unconfined flames; however, flames that were semi-confined (confinement cylinder with viewing window open) behaved much more sporadically due to an increase in turbulent swirling. Liftoff delays were also

15. SUBJECT TERMS
Combustion Control, Stability.

16. SECURITY CLASSIFICATION OF:			17. LIMITATION OF ABSTRACT	15. NUMBER OF PAGES	19a. NAME OF RESPONSIBLE PERSON
a. REPORT	b. ABSTRACT	c. THIS PAGE			Kevin Lyons
UU	UU	UU	UU		19b. TELEPHONE NUMBER 919-515-5293

Report Title

Turbulent Flame Stabilization Methods UsingConfinement, Diluents, and High-Potential Electric Fields.

ABSTRACT

Presented are three methods in controlling flame stability and enhancing flame control. The three methods that were observed were flame confinement, flame dilution with inert diluents, and high-potential electric field effects on flames. Flames that were under full confinement experienced similar liftoff trends to that of the unconfined flames; however, flames that were semi-confined (confinement cylinder with viewing window open) behaved much more sporadically due to an increase in turbulent swirling. Liftoff delays were also present in both the semi-confined and fully confined cases, such that a higher jet velocity is required to achieve initial liftoff from the fuel nozzle. In diluting methane and ethylene flames with nitrogen and argon it was observed that methane flames are more sensitive to dilution than ethylene flames. Also, ethylene flames were not a function of diluent type unlike methane flames. To incorporate the sensitivities of both methane and ethylene flames to diluent type, a correlation constant was incorporated into scaling methods that are used in predicting flame liftoff heights. Methane coefficients were higher in magnitude than ethylene flames, and the dependence of diluent type is present due to the values for methane being different. However, for ethylene flames, the correlation constants were similar in magnitude regardless of diluent type. Under the presence of a high-potential electric field it was determined that propane flame behavior is dependent on the polarity of the electric field. If the primary electrode was positively charged, the flame progressed toward blowout with increases in potential; however, when the primary electrode was grounded (secondary being positive), the flame reattached to the fuel nozzle with increasing potentials. By moving the primary electrode around various locations around the flame (near, mid, and far-field) it was observed that for positive configuration, the location of the electrode has no affect on the flame stability. Likewise, while in the grounded configuration, when the electrode was located in the far-field of the propane flame the flame was able to stabilize at higher potentials without reattaching to the fuel nozzle. Rapid progressions to either blowout or reattachment were observed, depending on the polarity of the electric field, when increasing the potentials. This was present even with incremental (100 V) increases of electric field potential. The hysteresis of the propane flame was greatly altered (while in the positive configuration) when the electric field was activated. With the electric field applied, the upper region of the typical hysteresis plot where the flame instabilities increase due to approaching blowout was not present. Also, flame lifted heights were determined to be higher while decreasing the jet velocity to observe the hysteresis regime. For the positive configuration, a flame discontinuity was observed after the primary electrode for several images.

ABSTRACT

HUTCHINS, ANDREW RYAN. Turbulent Flame Stabilization Methods Using Confinement, Diluents, and High-Potential Electric Fields. (Under the direction of Dr. Kevin Lyons).

Presented are three methods in controlling flame stability and enhancing flame control. The three methods that were observed were flame confinement, flame dilution with inert diluents, and high-potential electric field effects on flames. Flames that were under full confinement experienced similar liftoff trends to that of the unconfined flames; however, flames that were semi-confined (confinement cylinder with viewing window open) behaved much more sporadically due to an increase in turbulent swirling. Liftoff delays were also present in both the semi-confined and fully confined cases, such that a higher jet velocity is required to achieve initial liftoff from the fuel nozzle. In diluting methane and ethylene flames with nitrogen and argon it was observed that methane flames are more sensitive to dilution than ethylene flames. Also, ethylene flames were not a function of diluent type unlike methane flames. To incorporate the sensitivities of both methane and ethylene flames to diluent type, a correlation constant was incorporated into scaling methods that are used in predicting flame liftoff heights. Methane coefficients were higher in magnitude than ethylene flames, and the dependence of diluent type is present due to the values for methane being different. However, for ethylene flames, the correlation constants were similar in magnitude regardless of diluent type. Under the presence of a high-potential electric field it was determined that propane flame behavior is dependent on the polarity of the electric field. If the primary electrode was positively charged, the flame progressed toward blowout with increases in potential; however, when the primary electrode was grounded (secondary being positive), the flame reattached to the fuel nozzle with increasing potentials. By moving the

primary electrode around various locations around the flame (near, mid, and far-field) it was observed that for positive configuration, the location of the electrode has no affect on the flame stability. Likewise, while in the grounded configuration, when the electrode was located in the far-field of the propane flame the flame was able to stabilize at higher potentials without reattaching to the fuel nozzle. Rapid progressions to either blowout or reattachment were observed, depending on the polarity of the electric field, when increasing the potentials. This was present even with incremental (100 V) increases of electric field potential. The hysteresis of the propane flame was greatly altered (while in the positive configuration) when the electric field was activated. With the electric field applied, the upper region of the typical hysteresis plot where the flame instabilities increase due to approaching blowout was not present. Also, flame lifted heights were determined to be higher while decreasing the jet velocity to observe the hysteresis regime. For the positive configuration, a flame discontinuity was observed after the primary electrode for several images.

Turbulent Flame Stabilization Methods Using Confinement, Diluents, and High-Potential Electric Fields

by
Andrew Ryan Hutchins

A thesis submitted to the Graduate Faculty of
North Carolina State University
in partial fulfillment of the
requirements for the degree of
Master of Science

Mechanical Engineering

Raleigh, North Carolina

2014

APPROVED BY:

_____	_____
Kevin Lyons Committee Chair	Alexei Saveliev
_____	_____
Tiegang Fang	Stephen Terry

DEDICATION

To my parents (Robert and Renee Hutchins) and grandparents (David and Faye Harris), who without their love, support and discipline, none of this would have been possible.

BIOGRAPHY

Andrew Hutchins is a graduate student at North Carolina State University. Currently he is a graduate research assistant in the Reacting Flows and Turbulent Jets Laboratory in the Department of Mechanical and Aerospace Engineering. His research focus while a Master's student has been in turbulent flame stability. Andrew was born and raised in Elkin, NC where he graduated from Elkin High School in 2008. Following in his father's footsteps, Andrew enrolled into North Carolina State University to pursue a Bachelor of Science degree in mechanical engineering. After graduating in 2012, he promptly enrolled into graduate studies at North Carolina State University under the advisement of Dr. Kevin Lyons. Outside of graduate work, Andrew enjoys playing golf and spending time with his friends and fraternity brothers. In the future, Andrew will be pursuing a Doctoral Degree, as well as an MBA, at a to be determined institution.

ACKNOWLEDGMENTS

Andrew Hutchins would like to thank the following people who have helped along the way:

-Dr. Kevin Lyons, for his guidance and support

-Dr. Alexei Saveliev, Dr. Tiegang Fang, and Dr. Stephen Terry for serving on my committee

-Dr. Glenn Walker for serving as my graduate minor representative

-Dr. James Kribs for his assistance and training

-William Reach, Richard Muncey, and Galen Allen for assistance in data recording and setup design

The research reported in this thesis has been supported by the U.S. Army Research Office (Contracts W911NF0810142 and W911NF1210140) Dr. Ralph Anthenien, Technical Monitor, ARO.

TABLE OF CONTENTS

LIST OF TABLES

LIST OF FIGURES

CHAPTER 1: INTRODUCTION

1.1 Overview

Turbulent jet flames have been studied for several decades for their use in many industrial applications. Even with this tremendous amount of research time and funding being devoted to this important area, there are still countless problems and questions that still need to be answered. As energy and fuel costs continue to escalate, more and more methods are being developed to conserve fuel and money spent on wasted energy. One particular area in this research is studying how to increase flame control in order to utilize these jet flames in a predictable method. Below in Figure 1.1, is an image of a typical turbulent, lifted methane jet flame.

Figure 1.1: Partially Premixed Turbulent Methane Jet Flame

Further research into the area of turbulent jet flames could play a role in fuel conservation for the future of industries. The following paper describes three experimental investigations that could be used to increase flame control and stability.

1.2 Background

1.2.1 Confined Jet Flames

Stabilization of lifted flames is an important topic of discussion for many industrial applications. Studies have been conducted by Gollahalli et al. [1] and Terry and Lyons [2] to attempt to explain the liftoff effect that occurs, as well as hysteresis behavior. Diffusion flames are widely used in industry for turbines, boilers, and furnaces. It is known that jet flames experience blowout at various terminal velocities, which are dependent on the fuel type, ambient conditions, nozzle size, etc.

Turbulence/chemistry interactions have also been investigated extensively for several decades in parallel with many thermal-fluids studies. However, no definite delineation currently exists that fully describes the phenomenon completely. It may be noted, however, that widespread research has been conducted in the area of turbulent, lifted jet flames, in particular methane (CH_4) flames. These studies of turbulent lifted jet flames have been considered by Lyons [3] and Schefer et al. [4], in that the stoichiometric mixture of the fuel and oxidizer dominates near-field studies. Stabilization mechanisms of turbulent jets can be arranged into studies of fully premixed, partially premixed, and nonpremixed fuel and oxidizer. However, it can be debated that defining a jet as “fully” premixed is not completely accurate in that at the flame base there may be some instabilities (i.e. pressure gradients from

the fuel nozzle). The study involving various levels of flame confinement to be discussed involve these partially premixed flames. Thus no mixing is occurring in the fuel lines or in the coflow.

The traditional lifted jet flame phenomenon is altered when a confinement chamber separates the flame burner from the ambient surroundings. Two fundamental factors are introduced in (1) recirculation of the combustion products [5] and (2) a boundary layer that is formed at the edge of the confinement wall, as stated by Lawn [6]. Geometric cross-sections of the confinement device delegate the total effect that these mechanisms will have on the flame itself. As characterized by Cha and Chung [7], the liftoff height of a fully confined jet flame is directly related to the nozzle size and the jet velocity, similar to that of an unconfined jet.

It has been determined through extensive experimentation that the liftoff heights of these jets are linearly correlated to the jet velocity at the nozzle. However, this statement has only been proven to be true for unconfined jets, that is, jets that have free access to the ambient surroundings. Part of the report presented below will attempt to describe the flame behavior under various confined surroundings.

1.2.2 Flame Dilution

Understanding how turbulent jet flames will behave under the various flow conditions can permit the design of clean, stable, durable and efficient combustion systems, such as those listed previously. Studies on turbulent lifted flames have observed the fluctuations of the liftoff heights, variations of blowout limits, and hysteresis patterns [1-

2,4,8]. It is well known that turbulent jet flames liftoff from the fuel supply nozzle as the velocity of the fuel is increased beyond a critical point. As the flame experiences transition from attached to the nozzle to lifted, the luminosity of the flame is altered due to local air-fuel mixing and temperature variations.

A turbulent jet flame will experience three distinct phases before flame extinction is attained at high jet velocities. The first of these is an attached flame that is present while the flame is still anchored on the fuel nozzle (or fuel supply tube) at the flame base. The flame base is described as the lowest point of flame luminescence. As the fuel velocity is increased, the flame will leave the nozzle and stabilize at a certain height that is dependent on fuel velocity and other exterior parameters, such as non-reactive gas addition, coflowing (that is gas, most frequently air, flowing in parallel with jet velocity) annulus parameters [9-10] and flame confinement [7]. This lifted flame will oscillate at a mean lifted height until changes in local stoichiometry, jet velocities, coflow velocities, or combinations of these, alter the stabilization location [11]. In the final phase, flame blowout, the flame extinguishes shortly after the trailing diffusion flame vanishes [12]. A flame, however, can experience diverse phenomena in which the flame is extinguished directly after leaving the fuel supply nozzle [13-14]. This is known as flame blow off, which occurs when the flame cannot stabilize after lifting off from the nozzle and is immediately extinguished due to fuel velocities that do no permit stabilization of the flame in the given mixture fraction field.

The lifted flame, created by increasing the fuel flow rate or the non-reactive diluent gas flow rate, stabilizes at certain heights when keeping these flow rates constant; however,

at certain flow velocities the flame blows out due to the flame being driven past its flammability limit where it cannot stabilize. When the flame reaches this point, combustion can no longer occur and blowout (extinction) occurs. The flammability limit of the fuel being used is useful in predicting when the flame will blowout. Before the flame extinguishes due to high flow rates, it has been shown that the trailing diffusion flame generally disappears [12]. This blowout regime varies greatly with the makeup of the hydrocarbon fuel being tested. There have been many findings reported on the chemical reactions that occur while the flame is lifted and its behavior just before blowout occurs [15-16].

It has been experimentally and theoretically shown by Moore et al., Karbasi and Wierzba, and Chao et al. that the addition of inert gases to the fuel stream leads to a less stable turbulent diffusion flame [17-19]. Common diluents, such as diatomic nitrogen and carbon dioxide, have been well investigated and have proven to have significant effects on the liftoff behavior, as well as blowout limits, of methane jet flames [20]. However, most of these studies involve only the analysis of methane gas with additives, while few investigate the comparison of adding non-reactive gases to higher-order hydrocarbon fuels, such as ethylene [21]. This experimental study investigates the effect of diluting methane and ethylene jet flames with diatomic nitrogen and argon, independently. Phenomena to be investigated are the lifted flame stability between the two fuels, flame blowout regime, and inert diluent additive effects on flame luminosity, in particular around the flame base. In addition, a non-dimensional analysis has been performed to determine how previous studies correlate with the measured data. This involved the investigation of a non-dimensional

theoretical flame liftoff prediction that compares various diluent levels, as well as both fuels, for progressively increasing jet velocities.

1.2.3 Electric Fields and Flames

Studies involving the effects of electric fields on flame behavior have shown that flame stabilization parameters depend upon field strength, orientation, fuel type and other physical parameters [22-28]. The incorporation of a charged electrode within a flame medium (and a grounded fuel tube) impacts most of the typical parameters, such as the liftoff velocity [22], blowout/blowoff velocities [27], flame speeds [26,28], and temperature/species gradients [24-25]. These variances are expected, but difficult to predict, due to the large pool of ions already present in a flame, and the ions introduced near the electrode [29]. Thus, varying electrode location and polarity affects the flame in a complex manner. Utilizing an electric field to control flame behavior shows promise for stabilizing flames with higher jet velocities (i.e. flames nearing blowout at higher lifted heights) by using less fuel and preventing unburned fuel from being wasted.

Experiments involving turbulent flames have been reviewed by Pitts [30], and several theories that describe the stabilization mechanisms of lifted, turbulent flames have been proposed [31-36]. These stabilization mechanisms need to be investigated for configurations where a charged electrode impacts the ion concentrations already present in the flame [29], as well as body forces that can also effect flame shape and stability. In addition to lifted flame trends, the reattachment trends of the flame to the fuel nozzle should be investigated. This involves studying the hysteresis regime where the flame remains lifted after decreasing

the jet velocity past the initial liftoff velocity. Past studies have investigated this hysteresis regime [1-2,9,37], however, none have studied the hysteresis regime of a flame in the presence of a high-potential electric field. This paper will compare the flame hysteresis regime with no field to those witnessed with increasing electric field potential.

Various other external influences such as an ambient air coflow [9-10,18,38], jet confinement/recirculation [5,7,39], inert dilution [18,40-44], and enrichment [45-46] impact flame behavior. Lee et al. [22] found that an alternating current applied to a turbulent propane flame decreases liftoff height and delays liftoff, thus increasing flame stability; however, for direct current the impact on the flame stability was minimal. Also, it was determined that for lower voltages (less than 1 kV) the liftoff velocity increased linearly for increasing potentials. The larger influence of AC in comparison to DC when observing the detachment velocity (linear increase for voltages less than 2-4 kV), reattachment velocity (linear increase), and propagation speed (increase) was verified by Kim et al. [27].

In addition, it is well known that a pulsating electric field has a much different effect on flame behavior when compared to a constantly applied field. Garanin et al. [28] found that for laminar modes a periodically pulsating electric field increased the burning rate and that during transition regimes the constantly applied electric field affected combustion stability. Bak et al. [47] observed flame behavior for both lean premixed and diffusion flames while implementing a nanosecond repetitive pulsed discharge. It was found that for lean premixed conditions, the flame propagation did not vary much from that expected in the corresponding flammable region in the situation with zero field applied. For diffusion flames, the location of

the corona discharge was optimal for flame stabilization when it was located where fuel/air mixtures were within flammability limits locally.

This study describes an experimental investigation involving a high-potential electric field from a charged ring electrode. The location of the charged ring is varied with initial flame liftoff height (corresponding to the initial jet velocity) as well as the polarity of the copper ring (positive or grounded with opposite polarity on the fuel nozzle). Flame behavior (liftoff, blowout, hysteresis, etc.) and structure have been studied and presented for jet velocities with Reynolds Number varying from 430 to 920. Discussions are also included on how the hysteresis region of flame nozzle reattachment is varied with the introduction of a charged electrode. The findings of the paper describe a variety of effects of the various polarity electrodes on flame stability, and included are discussions for potential applications of the electric field approach to flame anchoring and manipulation.

1.3 Objectives

In designing and experimenting with various methods of flame control, several objectives were kept in mind. These objectives focused around improving flame stability for uses in industrial applications, such as boilers, furnaces, etc. Some specific goals were as follows:

1. Determine if confining a methane jet flame (with the presence of ambient coflow) would increase flame stability and decrease turbulent swirling.
2. Determine how a partially confined methane flame would behave in comparison to a fully confined methane jet flame.

3. Determine if there are better methods in predicting non-dimensional liftoff heights of diluted methane and ethylene jet flames.
4. Determine if methane and ethylene flame stability is a function of the diluent type and not just the amount of diluent used.
5. Determine if modifications are necessary to well known empirical flame liftoff predictions.
6. Determine if the polarity of a high-potential electric field makes a lifted propane flame behave in various manners.
7. Determine how the hysteresis curve is shifted if a high-potential electric field is present in the flame medium.
8. Determine if any flame holes/discontinuities are present that could lead to better combustion control.

10

CHAPTER 2: STABILIZATION MECHANISMS OF CONFINED, TURBULENT FLAMES

Excerpts from: Andrew Hutchins, James Kribs, Richard Muncey, and Kevin Lyons, Assessment of Stabilization Mechanisms of Confined, Turbulent, Lifted Jet Flames: Effects of Ambient Coflow, ASME 2013 Power Conference, ©ASME 2013

2.1 Abstract

The aim of this investigation is to determine the effects of confinement on the stabilization of turbulent, lifted methane (CH_4) jet flames. A confinement cylinder (stainless steel) separates the coflow from the ambient air and restricts excess room air from being entrained into the combustion chamber, and thus produces varying stabilization patterns. The experiments were executed using fully confined, semi-confined, and unconfined conditions, as well as by varying fuel flow rate and coflow velocity (ambient air flowing in the same direction as the fuel jet). Methane flames experience liftoff and blowout at well known conditions for unconfined jets, however, it was determined that with semi-confined conditions the flame does not experience blowout, even at maximum flow rate potentials. Instead of the conventional unconfined stabilization patterns, an intense, intermittent behavior of the flame was observed. This sporadic behavior of the flame, while under semi-confinement, was determined to be a result from the restricted oxidizer access as well as the asymmetrical boundary layer that forms due to the viewing window. While under full confinement, the flame behaved in a similar method as while under no confinement (full

ambient air access). The stable nature of the flame while fully confined lacked the expected change in leading edge fluctuations that normally occur in turbulent jet flames. These behaviors address the combustion chemistry (lack of oxygen), turbulent mixing, and heat release that combine to produce the observed phenomena.

2.2 Experimental Setup

The fuel that was used in all the tests was methane (CP Grade, 99% Pure), which flowed through a 3.5 millimeter diameter nozzle. The flow was fully developed (length to diameter ratio greater than 10) for each of the three confinement cases. The shrouding coflow air was driven by a Magnetek (model 9467) centrifugal blower across the 150 millimeter annulus. This ambient coflowing shroud has a well-developed flat (top-hat) profile normal to the flow velocity across the entire annulus. The velocity of the ambient coflow was measured using a TSI hot wire anemometer, and the methane volumetric flow rate was measured/controlled using an Advanced Specialty Gas Equipment Series 150 Flowmeter. Figure 2.1 illustrates the burner used in each of the three apparatuses.

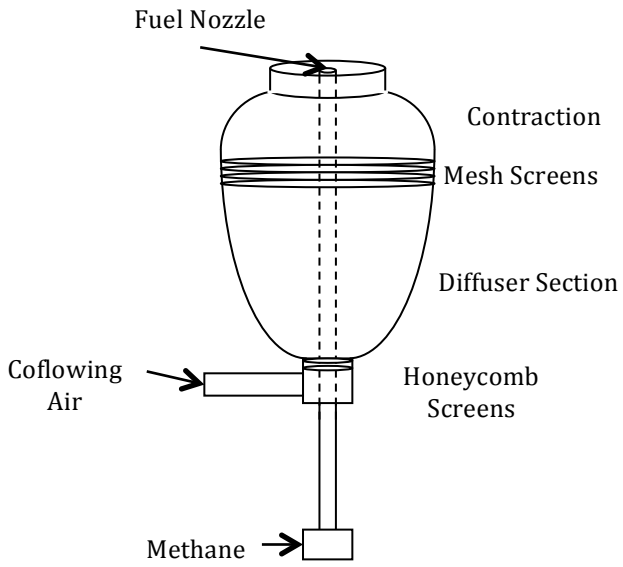

Figure 2.1: Coaxial Burner Apparatus

The open burner illustrated above was used to determine the stabilization limits for the flame under no confinement. For the confinement and semi-confinement experiments a stainless steel cylinder was used to entrap the methane jet flame. This confinement cylinder was 122 centimeters in height and had an outer diameter of 16.75 centimeters. The thickness of the cylinder wall was 0.4 centimeters. There also existed a viewing window (used for the semi-confined apparatus and covered with Lexan for the fully confined apparatus) that was 6.75 centimeters from the cylinder bottom and measured to a height of 101 centimeters. This viewing window was 2.9 centimeters wide, which is small to limit the flame's access to ambient air Figure 2.2 shows the stainless steel confinement cylinder.

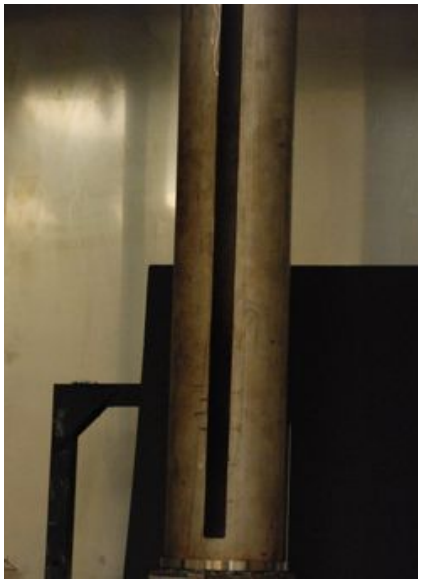

Figure 2.2: Stainless Steel Confinement Cylinder

Images were taken using a Nikon D80 Digital SLR camera with an 18-105 millimeter Nikkor Lens. Fuel volumetric flow rate, coflow velocity, and confinement cases were all varied for a total of nine various conditions. Each of these cases was photographed 10 times and an average liftoff height was analyzed. These liftoff heights were measured with Adobe Photoshop by using pixel to distance conversion. The lowest level of flame luminosity was used as the stabilized height for each flame image and was measured from the fuel nozzle.

2.3 Results and Discussion

Three various confinement conditions were used to surround the methane flame, as well as three coflow levels (zero coflow, low coflow velocity at 0.18 m/s, and high coflow velocity at 0.38 m/s) and various methane volumetric flow rates. A value can be determined that represents the total effect from the fuel jet and coflowing shroud. This is known as the

effective velocity, and is the overall velocity resulting from the combination of the fuel velocity and the coflow velocity. This formulation is given as

$$U_{eff} = U_f + C\sqrt{\frac{\rho_{coflow}}{\rho_{fuel}}}U_{coflow} \quad (1)$$

where U_f is the jet fuel velocity, ρ_{coflow} is the density of the ambient coflowing air, ρ_{fuel} is the density of the fuel, U_{coflow} is the velocity of the ambient coflowing air, and C is an experimental constant of 40, as in Kumar et al. [48]. Below in Table 2.1 are the 18 various cases used, as well as the effective velocities.

Table 2.1: Experimental Levels Used in Confinement Testing

Methane Velocity (m/s)	**Coflow Velocity (m/s)**	**Effective Velocity (m/s)**
6.70	0.00	6.70
16.51	0.00	16.51
25.75	0.00	25.75
35.56	0.00	35.56
45.87	0.00	45.87
57.39	0.00	57.39
6.70	0.18	16.37
16.51	0.18	26.18
25.75	0.18	35.42
35.56	0.18	45.23
45.87	0.18	55.53
57.39	0.18	67.06
6.70	0.38	27.11
16.51	0.38	36.92
25.75	0.38	46.16
35.56	0.38	55.97
45.87	0.38	66.27
57.39	0.38	77.79

The iterations above were used for the unconfined, semi-confined, and fully confined cases for a total of 54 various conditions. It was determined that the unconfined and fully confined conditions resulted in similar stabilization patterns. However, while under semi-confinement (i.e. open window) the flame behaved sporadically and had a lower overall liftoff height. This sporadic behavior is directly related to the small viewing window in the confinement cylinder that results in turbulent swirling (increased mixing) near the flame. While most of the flame is restricted to only a small amount of oxidizer, the front of the flame has free access to the excess air. Also, from Figure 2.3 it can be seen that the flame luminosity varies between each of the three confinement conditions. The semi-confined case results in more orange resulting from soot formation, which may be directly linked to the sporadic behavior of the flame (enhanced turbulent mixing leading to higher temperatures). In addition, the swirling that develops from the open viewing window could result in a reduction in the convective heat transfer rate. The radiation that occurs from the flame is also being reflected back due to the confinement cylinder. This results in the flame burning at a much higher temperature in the semi-confined and fully confined cases. This higher flame temperature is related to the equivalence ratio between the fuel and oxidizer. The fully confined condition results in less soot formation. Figure 2.3 shows a comparison of the methane jet flame with constant fuel velocity and coflow velocity, but with varying confinement conditions.

Figure 2.3: Methane Jet with Various Confinement Conditions

Figure 2.4 illustrates the relationship between the calculated effective velocity and the methane jet flame liftoff heights. It may be noted that the expected trend of increasing liftoff heights with increasing fuel/coflow velocities is present. The trends of the unconfined and fully confined setups follow a relatively similar pattern, while the semi-confined setup experienced lower liftoff heights. These lower liftoff heights are present in the semi-confined case due to the near stoichiometric environment with the reduction in oxidizer access. Additionally, one possible explanation to the similar trends of the unconfined and fully confined cases could be that the unconfined case burn fuel lean while the fully confined case

burns fuel rich. The curve that explains this phenomenon is a normalized distribution of the adiabatic flame temperature versus the stoichiometric ratio. The unconfined condition allows for the flame to liftoff at a lower effective velocity than that of the semi-confined and fully confined cases. The initial spike in liftoff generated by the semi-confined and fully confined cases is explained by the more fuel rich environment developed by the confinement walls.

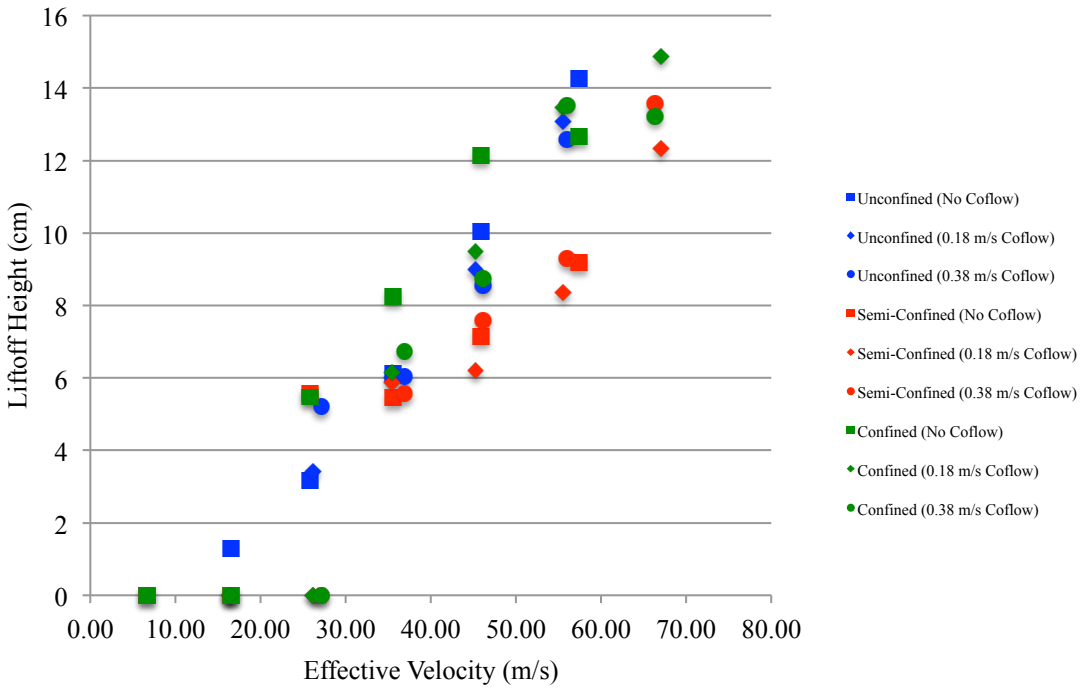

Figure 2.4: Comparison of Effective Velocity and Liftoff Heights

The theory discussed by Ogami and Kobayashi [49] assists in explaining why the methane flame stabilizes at lower liftoff heights while under semi-confinement than that of unconfined or full confinement. The direct correlation between laminar flame speeds and

turbulent flame speeds is well known. Thus, it can be stated that since the unconfined condition is burning fuel-lean the flame will liftoff at lower fuel velocities than that of the semi-confined apparatus. However, it can be seen that initially the fully confined case also lifts off at higher velocities than that of the unconfined case. This “liftoff delay” can be explained by the much higher stoichiometric fuel-to-air ratio resulting in a spike in the liftoff height. After this initial spike, the flame experiences a stabilization period where the trend closely follows that of the unconfined case.

It is important to note that these trends are strictly for the effective velocity and not solely the methane jet velocity from the nozzle. Trends with just the liftoff height and the methane jet volumetric flow rate are altered in that coflow does not “normalize” the data sets. Figures 2.5. 2.6, and 2.7 illustrate the trends observed when separating each coflow velocity level into their own plot and focusing only on the methane jet volumetric flow rates. These trends clearly demonstrate that for each coflow velocity level the semi-confined apparatus consistently experienced a lower flame liftoff height than that of unconfined and the fully confined cases.

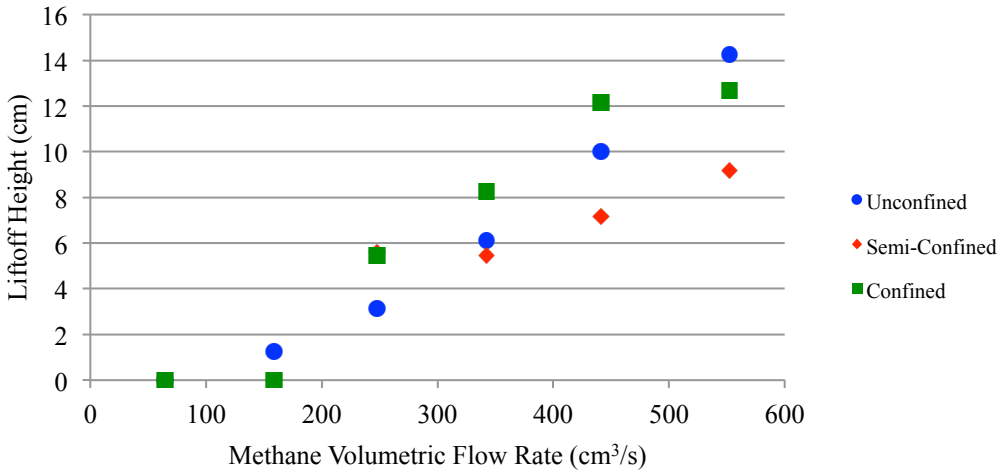

Figure 2.5: Methane Flame Liftoff Heights with no Coflow

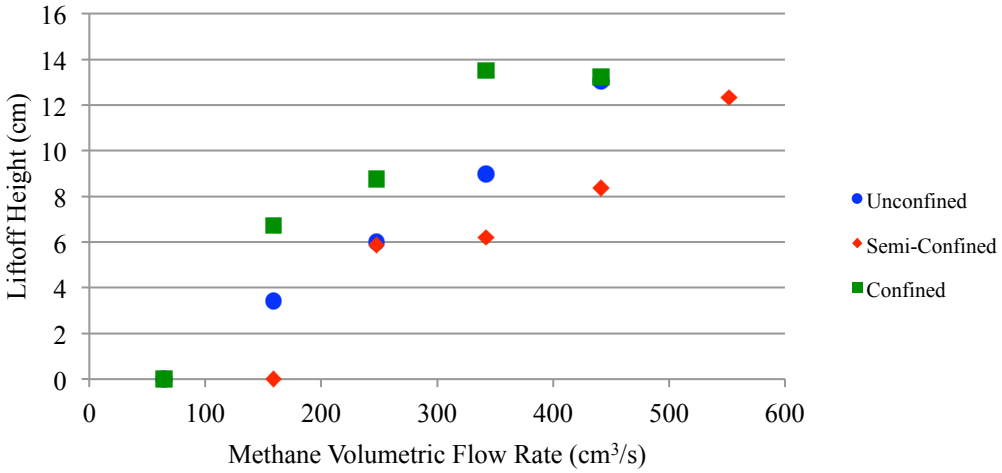

Figure 2.6: Methane Flame Liftoff Heights with 0.18 m/s Coflow

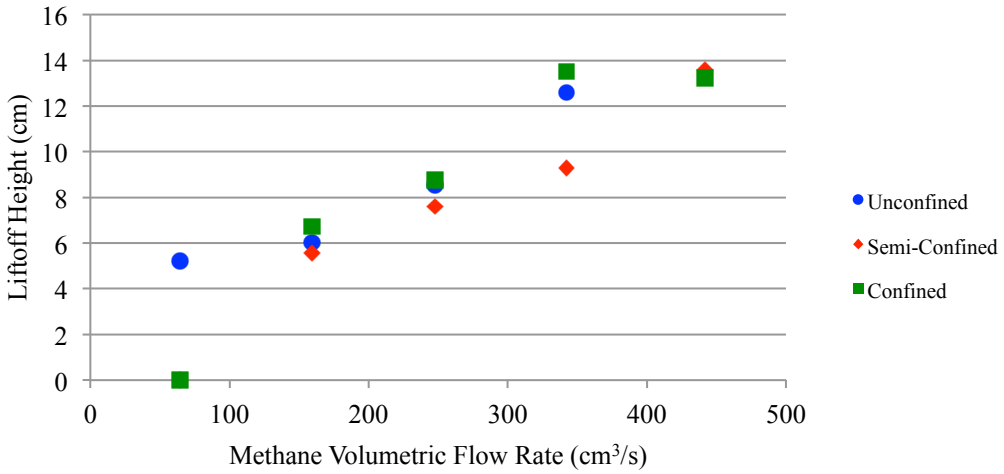

Figure 2.7: Methane Flame Liftoff Heights with 0.38 m/s Coflow

It is proven to be difficult to reach blowout while under either of the confined conditions. This could be attributed to the fact that both the semi-confined and fully confined cases produce a more fuel-rich environment than that of the unconfined case (as stated earlier). Instead of achieving blowout, the fully confined case resulted in a stable flame at much higher jet velocities than that of unconfined jet flames. Attempts at reaching blowout only resulted in a larger flame within the confinement cylinder. Further attempts to reach blowout would require an extended confinement device beyond the scope of the present study.

The combustion length of these jets can be directly related to the mixing of the fuel and air within the confinement cylinder, as proposed by Thring and Newby [50]. This mixing is dependent only on the size of the confinement chamber that is entrapping the flame. It may also be noted that in each of the three cases the flame will act as if it is unconfined until the

flame reaches the interior wall of the confinement cylinder as in Guruz et al. [51]. It can be seen from Figure 2.4 that the flame stabilizes at similar liftoff heights for each of the three cases for lower effective velocities. This theory explains why the jets continue to separate as the effective velocity is increased.

2.4 Conclusions

Observing and comparing the results from each of the three confinement cases resulted in the following conclusions:

1. Stabilization mechanisms greatly differ when restricting a methane jet flame from its ambient surroundings (i.e. reduction in oxidizer from ambient surroundings to the combustion chamber).
2. Both the fully confined and unconfined experiments resulted in flames that had similar behavior, while semi-confined methane jet flames behaved much more sporadic.
3. Comparing effective velocity to the liftoff height for each confinement case illustrated that the fully confined and unconfined conditions had very similar trends, while the semi-confined apparatus resulted in jet flames that stabilized at a lower liftoff height.
4. A “liftoff delay” is present in both the semi-confined and fully confined cases where a higher jet velocity is required for the flame to detach from the fuel nozzle.

CHAPTER 3: EFFECTS OF DILUENTS ON METHANE AND ETHYLENE JET FLAMES

Excerpts from: Andrew Hutchins, James Kribs, and Kevin Lyons, Effects of Diluents on Lifted Turbulent Methane and Ethylene Jet Flames, ASME J. Energy Resour. Technol. (IN PREPARATION), 2014

3.1 Abstract

This study focuses on the effects of diluents on the liftoff of turbulent, partially premixed methane (CH_4) and ethylene (C_2H_4) jet flames for potential impact in industrial burner operation. Both fuel jets were diluted with nitrogen and argon in separate experiments, and the flame liftoff heights were compared for a variety of flow conditions. Methane flames have been shown to liftoff at lower jet velocities and reach blowout conditions much more rapidly than ethylene flames. Diluting ethylene and methane jets with nitrogen and argon, independently, resulted in varying trends for both fuels. At low dilution levels (5% by mole fraction), methane flames were lifted at similar heights, regardless of the diluent type; however, at higher dilution levels (10% by mole fraction) the argon diluent produced a flame which stabilized farther downstream. Ethylene jet flames proved to vary less in liftoff heights depending on diluent type. Significant soot reduction with dilution is witnessed for ethylene and methane flames, in that flame luminosity alteration occurs at the flame base at increasing levels of argon and nitrogen dilution. The increasing dilution levels also proved to decrease the liftoff velocity of the fuel, as well as decrease the radial position

of the flame. Theoretical analysis showed little variance between liftoff heights in ethylene flames for the various inert diluents, while methane flames proved to be more sensitive to diluent type. This sensitivity is attributed to the more narrow limits of flammability of methane in comparison to ethylene, as well as the much higher flame speed of ethylene flames.

3.2 Experimental Setup

Fuels that were utilized were ethylene (CP Grade, 99.5% Pure) and methane (CP Grade, 99% Pure), while the diluents consisted of pure diatomic nitrogen and argon gases. The fuel nozzle measured 3.5 millimeters and was long enough to ensure that fully developed turbulent flow as present at the nozzle exit (length to diameter ratio much greater than ten). The volumetric flow rates of the fuel and inert gas were measured and regulated using an Advanced Specialty Gas Equipment Series 150 Flowmeter, and the images were taken using a Nikon D80 Digital SLR camera with an 18-105 millimeter Nikkor lens. Figure 3.1 gives an illustration of the apparatus described.

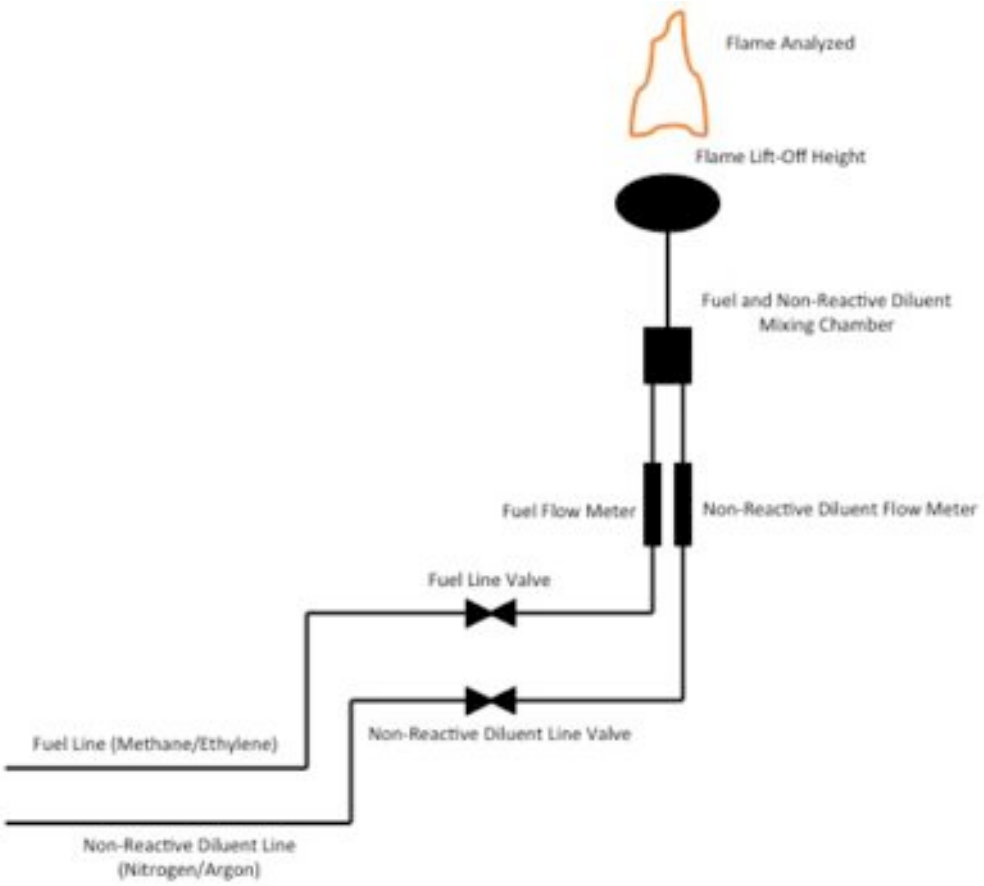

Figure 3.1: Apparatus for Diluent Experiments

Using the apparatus illustrated in Figure 3.1, each of the scenarios of fuel flow rate and inert gas dilution flow rate were photographed multiple times for statistical analysis purposes. Utilizing each fuel separately with one of the two inert diluents being applied individually to the fuel, the liftoff heights of each of the flames were measured and an average liftoff height was determined from the ten measured liftoff heights for each case. The various scenarios consisted of varying the mole fraction at the nozzle exit of the inert diluent

at levels of 0%, 5%, 10%, and 20% by total mole fraction of the jet flow (the balance of the jet flow being the fuel of interest). Each average liftoff height was then plotted to determine the trend in comparison between stabilization heights of methane and ethylene and various levels of nitrogen and argon dilution. This experimental data was then compared to theoretical predictions formulated by Broadwell et al. [35], and modifications to the scaling mechanisms in [35] are proposed for the cases examined.

3.3 Theory

In studying a lifted flame, many theoretical studies have attempted to describe the phenomena that occur. A topic of specific interest is how to incorporate the mixing of inert gas with that of the fuel. An investigation carried out by Yumlu [52] in 1968 studies the laminar flame speed in these types of mixtures. Using Equation (2) given below, the "corrected" flame speeds were determined for both methane and ethylene, and for their corresponding mixtures percentages. The formulation given is

$$S_{u,m}^2 = (1-\alpha)S_{u,fuel}^2 \tag{2}$$

where $S_{u,m}$ is the burning speed of the mixture, α is the mass fraction of the inert diluent within the mixture, and $S_{u,fuel}$ represents the burning velocity of the pure fuel jet. However, by adding inert diluents to the fuel the temperature downstream is decreased. Thus, using the Arrhenius law, Equation (3) from Yumlu can be altered to

$$S_{u,m} = [1-\alpha]^{1/2} S_u^0 \exp\left(-\frac{E_a}{R}\left(\frac{1}{T_b}-\frac{1}{T_b^0}\right)\right) \tag{3}$$

where S_u^0 is the burning velocity of the pure fuel, E_a is the activation energy, R represents the universal gas constant, T_b is the mixture burning temperature (adiabatic flame temperature of

the mixture), and T_b^0 is the burning temperature of the pure fuel (adiabatic flame temperature of the pure fuel jet) [52]. The laminar flame speeds for pure methane and ethylene jets are 0.39 m/s and 0.75 m/s, respectively [53].

Utilizing these equations from Yumlu, the flame liftoff height dependence (x_l) for mixtures can be predicted using flame liftoff scaling given as

$$x_l \sim \left(u_0 d_0 \left(\frac{\rho_0}{\rho_\infty} \right)^{1/2} \left(\frac{\kappa}{S_{u,m}^2} \right) \right)^{1/2} \tag{4}$$

where u_0 is the local velocity, d_0 is the local diameter, ρ_0 is the pure fuel density, ρ_∞ is the surrounding air density, and κ is the thermal diffusivity [35]. This scaling is non-dimensionalized to determine the liftoff predictions for both fuels and the various scenarios of diluent levels. The non-dimensional formulation is given below in Equation (5).

$$\frac{x_{l,y\%}}{x_{l,0\%}} = \frac{\left(u_0 \rho_0^{1/2} \frac{1}{S_{u,m}^2} \right)_{y\%}}{\left(u_0 \rho_0^{1/2} \frac{1}{S_{u,m}^2} \right)_{0\%}} \tag{5}$$

The notation of y% represents the various mole fraction percent levels used in each scenario. The variance in the equation compares a certain dilution level (numerator) to the control case of pure fuel jet (denominator). The non-dimensional scaling predictions of flame liftoff for the various scenarios of inert gas dilution are compared to the experimental findings presented in Figures 3.6 and 3.7.

3.4 Results

Figures 3.2 and 3.3 give visual comparisons of varying fuels with different mole fraction dilution levels of inert gases. These visuals represent various incandescent trends as

well as flame liftoff variances with nitrogen and argon diluents. Investigations of ethylene flames produced similar results when diluting the pure fuel jet with various concentrations of nitrogen and argon. Figure 3.2(a) illustrates the pure ethylene flame in comparison to high levels of nitrogen dilution (20% by mole fraction), while Figure 3.2(b) gives the pure ethylene flame in comparison to high levels of argon dilution (20% by mole fraction). For both Figures 3.2(a) and 3.2(b) the fuel jet velocity is held constant at 49.73 m/s for the 0% dilution cases. However, the combined jet velocity is greater for the 20% dilution cases due to the addition of the inert gases.

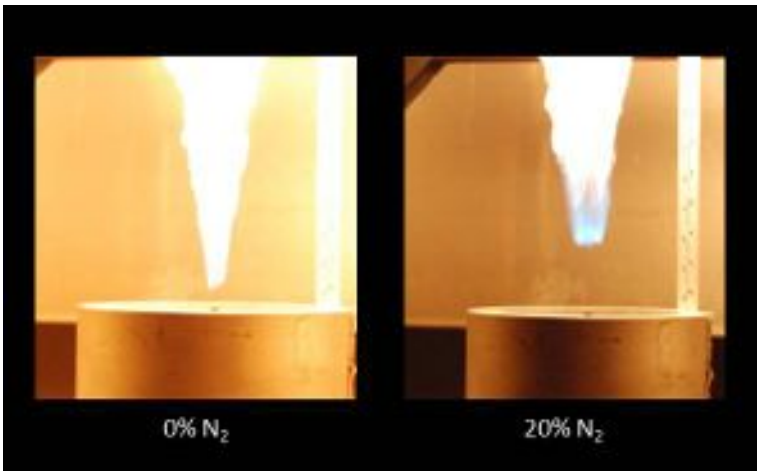

Figure 3.2(a): Pure Ethylene Flame Luminosity in Comparison to High Level (20% by Mole Fraction) Dilution of Nitrogen

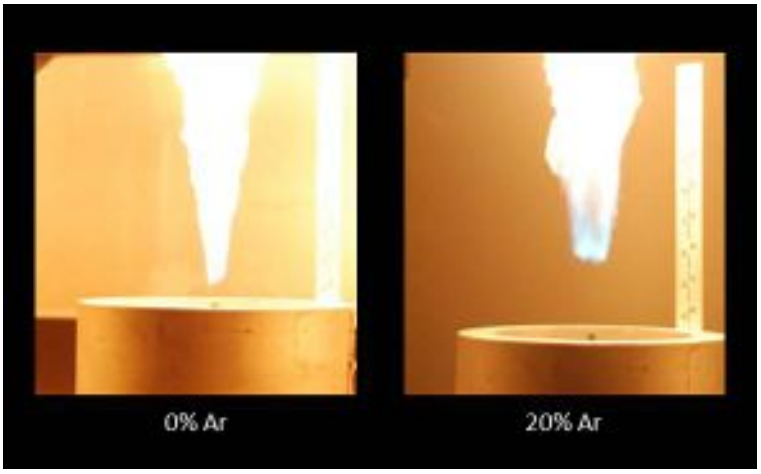

Figure 3.2(b): Pure Ethylene Flame Luminosity in Comparison to High Level (20% by Mole Fraction) Dilution of Argon

For the nitrogen-diluted case in Figure 3.2(a), the combined jet velocity at 20% dilution is 63.71 m/s, and for the argon-diluted case in Figure 3.2(b) the combined jet velocity at 20% dilution is 58.94 m/s. What should be noticed from these comparisons are the decreases in soot incandescence near the upstream portion of the reaction zone. The images illustrate that both nitrogen and argon dilution decrease soot incandescence at the flame base at similar levels for high levels of dilution (20% by mole fraction). Both inert gases reduce the blackbody soot radiation that saturates the flame base, allowing the blue flame luminosity to become visible. Figure 3.3(a) and 3.3(b) give a similar comparison for methane jets; however, the pure methane flame is compared with 5% by mole fraction dilution cases for nitrogen and argon, respectively. A lower dilution level is shown due to the instabilities that are present with high dilution levels in methane flames (metastable flame liftoff and flame blowout/blowoff). It can be seen in Figure 3.3(a) and 3.3(b) that diluting methane flames has

little effect on the flame luminosity. This varies from the diluted ethylene flames in that only the near-field soot incandescence is lowered due to the increase in inert gas dilution.

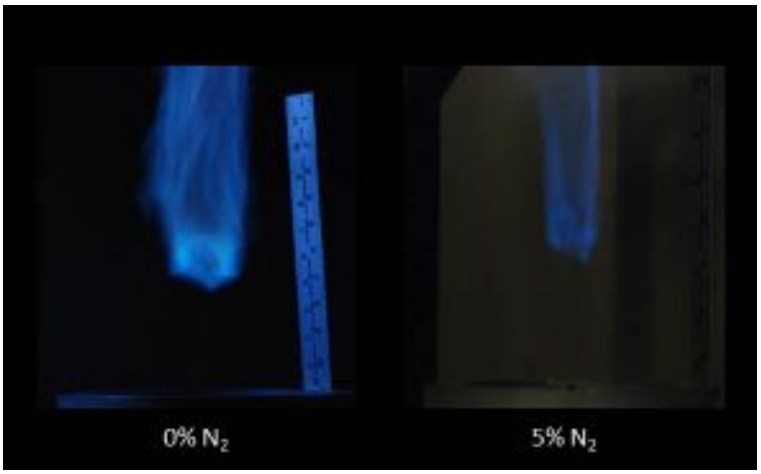

Figure 3.3(a): Pure Methane Flame Luminosity in Comparison to Low Level (5% by Mole Fraction) Dilution of Nitrogen

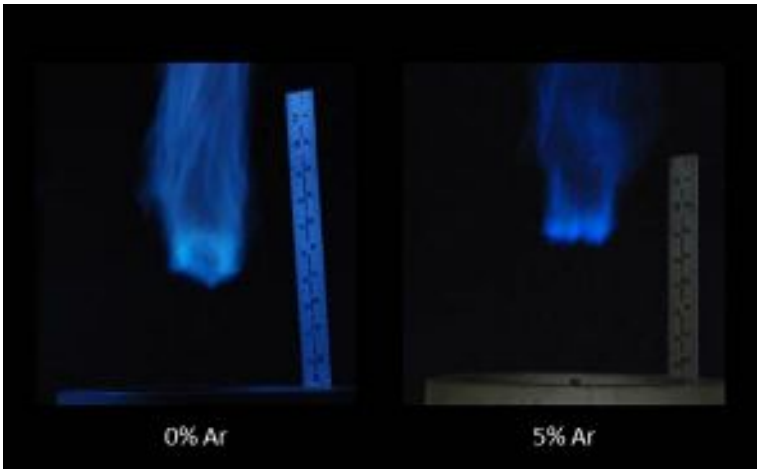

Figure 3.3(b): Pure Methane Flame Luminosity in Comparison to Low Level (5% by Mole Fraction) Dilution of Nitrogen

For ethylene, when both levels approach 20% by mole fraction, the flames experience similar levels of soot incandescence and flame luminosity for both diluents (Figures 3.2(a) and 3.2(b)). The methane comparison in Figures 3.3(a) and 3.3(b) show similar flame luminosity across the flame, as well as low soot incandescence. The rapid blowout/metastable phenomena that occur with dilution levels above 5% mole fraction for methane are attributed to the smaller flammability limit of methane in comparison to that of ethylene flames, as well as the higher flame speed of ethylene.

Initial results illustrate trends for fuel liftoff heights with increasing fuel velocity and inert diluent concentration. Each scenario of diluted methane and ethylene flames was plotted to observe various liftoff heights for changes in behavior at various dilution levels and fuel velocities. Figure 3.4 gives the plot of flame base heights from the fuel nozzle against the corresponding fuel velocities at the nozzle. This plot shows the liftoff heights for both nitrogen and argon dilution levels with methane.

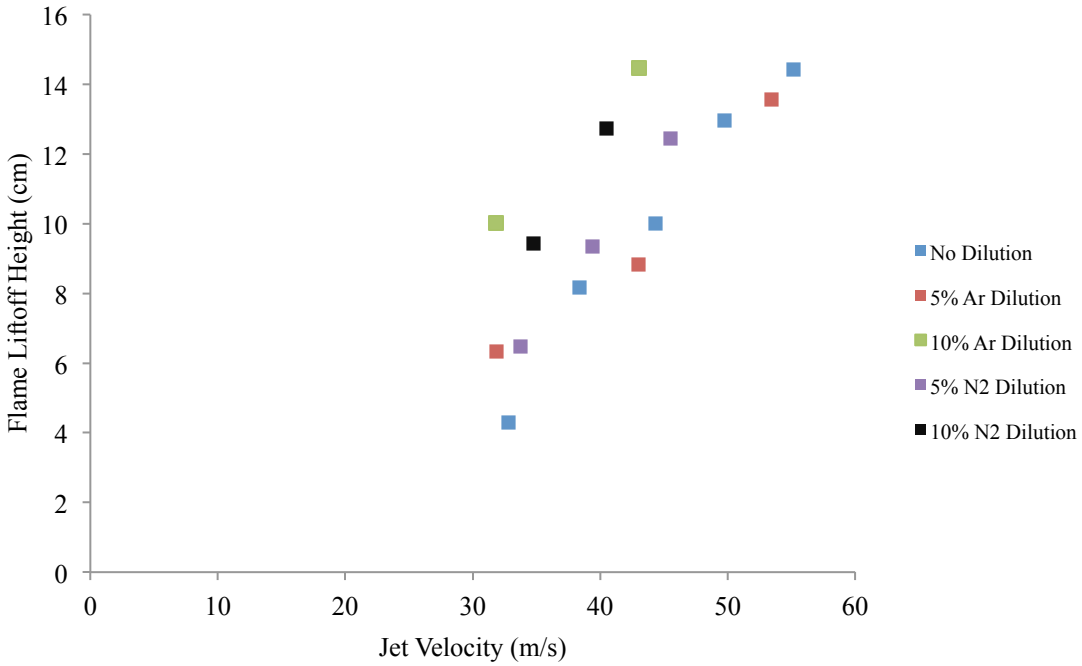

Figure 3.4: Methane Jet Flame Liftoff Heights for Argon/Nitrogen Dilution

It should be noted that even small dilution mole fractions affect the liftoff of the flame drastically. The effect of nitrogen dilution on the lifted methane flame is much greater than that of the argon diluted scenario at lower levels of dilution, and argon proved to be more significant (that is, force the flame to liftoff higher) at higher levels of dilution. This variance in liftoff phenomenon addresses the chemical makeup of the two inert gases in that argon is stable in nature and thus, being monatomic, there are no molecular bond energies. In contrast, diatomic nitrogen is bound by a much higher energy covalent triple bond energies. In comparing specific heats of nitrogen and argon, one finds that argon has a specific heat of ~0.52 KJ/(kgK), while nitrogen has a specific heat of ~1.04 KJ/(kgK). These variances in specific heats also attribute to the differences in liftoff in methane jets and not as much in

ethylene jets due to the much higher adiabatic flame temperature of ethylene. An additional explanation behind this phenomenon is the much higher flame speed that exists with ethylene flames (approximately twice that of methane flames). This observation is addressed later when examining the theoretical scaling of the flame liftoff heights, while the observed trend is presented in Figure 3.5.

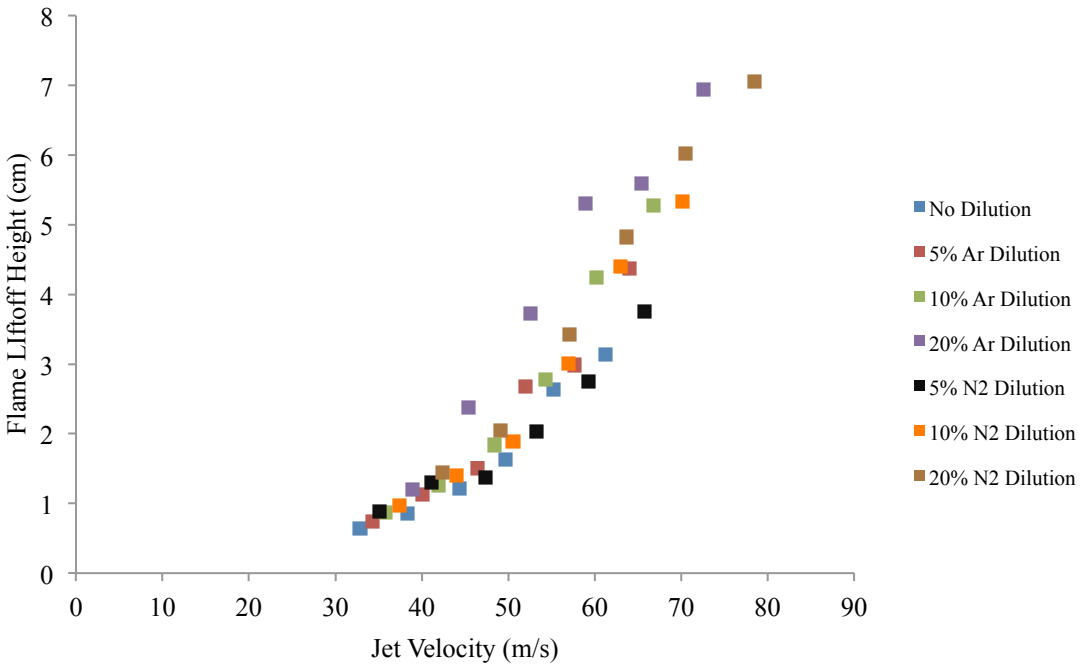

Figure 3.5: Ethylene Jet Flame Liftoff Heights for Argon/Nitrogen Dilution

In comparison to Figure 3.4, with methane it can be seen that many fewer experimental points were determined due to the methane flame reaching blowout at much lower jet velocities than that of the ethylene flame. In addition, it can be seen that the

ethylene flame requires a higher nozzle jet velocity to cause the flame to liftoff from the nozzle. To compare trends between different inert gases at the same levels of mole fraction dilution, the liftoff heights were non-dimensionalized and compared with the fuel mass flow rates. The mass flow rates are used to compare the non-dimensional heights due to the varying jet velocities between levels of diluent levels. By examining the mass flow rate of the fuel instead of the overall jet velocity, each of the levels of dilution fall in line, with respect to the x-axis. Thus, it is easier to compare the non-dimensional liftoff heights across each level of dilution. Observing Figure 3.4 and 3.5, it can be seen that, unlike the methane liftoff progression, the ethylene data at the lower positions are closely related. Figures 3.6 and 3.7 give the non-dimensional liftoff heights for methane and ethylene, respectively. Referring to Figure 3.6, it can be seen for methane jets that the sensitivity of the flame is great when comparing the experimental non-dimensional liftoff heights to that of the non-dimensional flame liftoff scaling. However, for the ethylene non-dimensional liftoff progressions in Figure 3.7 the values differ after 5% dilution levels of argon and nitrogen.

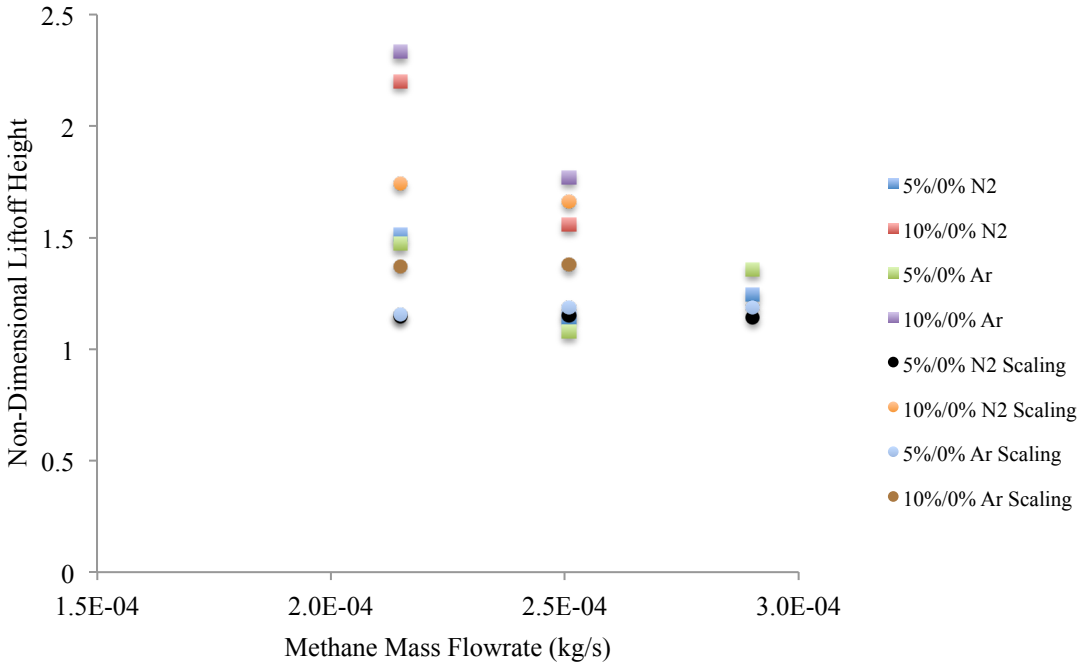

Figure 3.6: Non-Dimensional Methane Flame Liftoff Heights for Nitrogen/Argon Dilution and Comparing Experimental to Scaled (Empirical) Results

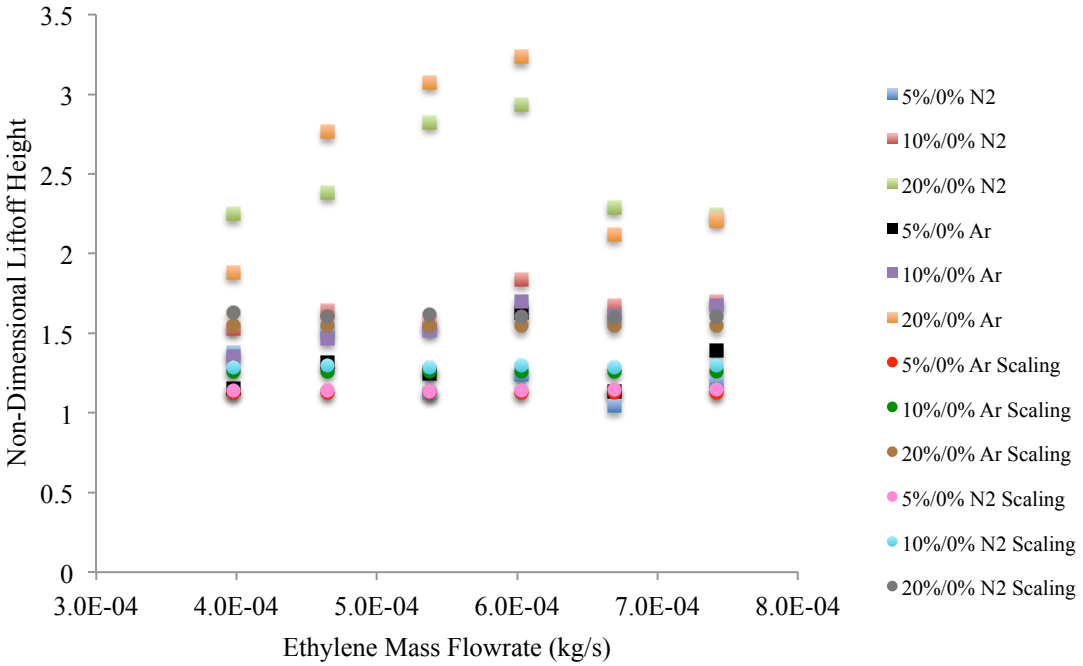

Figure 3.7: Non-Dimensional Ethylene Flame Liftoff Heights for Nitrogen/Argon Dilution and Comparing Experimental to Scaled (Empirical) Results

Referring to Figures 3.6 and 3.7, it can be seen that for methane jets the sensitivity of the flame is great when comparing the experimental non-dimensional liftoff heights to that of the non-dimensional flame liftoff scaling. In Figure 3.6, for methane, the 5% dilution levels of nitrogen and argon are similar in trend and non-dimensional value; however, when the dilution level is increased to 10% by mole fraction the points are separated. For ethylene, shown in Figure 3.7, the correlations are quite different. The experimental non-dimensional data suggests that the liftoff height for turbulent ethylene flames is less a function of inert diluent type, but instead more dependent on the diluent mole fraction. This varies greatly from the data given from the methane, in that for turbulent methane jets the liftoff height is a

function of *both* inert diluent type and diluent mole fraction. While diluting both methane and ethylene jets give similar variations in flame luminosity with increasing levels of inert diluents regardless of diluent type, the liftoff progressions with increasing levels of diluents varies between the two fuels and the diluent being applied. Claiming that methane flame liftoff height is a function of both inert diluent and diluent mole fraction addresses the much lower flame speed of methane in comparison to ethylene. Thus, ethylene is not influenced as much by the diluents due to the speed/intensity at which ethylene flames burn.

3.5 Discussion

The observations regarding flame liftoff of methane ethylene flames described validate that positions that methane flames are much more sensitive (that is, affected in a greater fashion) to dilution by inert gases than ethylene flames with the same/similar conditions. Observing the non-dimensional analysis of the experimental and theoretical results, it can be seen that a correlation constant might be introduced into Equation (5) to shift the theoretical data to approximately match the experimental results. This correlation constant (C_H) is a ratio of the non-dimensional theoretical liftoff heights to the non-dimensional experimental height.

Average values were determined for both methane and ethylene diluted jet flames. For the methane jets, the two inert diluents resulted in two correlation constants that vary greatly. This is due to the different effects that nitrogen and argon dilution have on methane flames. The average correlation constant for nitrogen diluted methane jets was determined to be 0.91, while the constant for argon diluted methane jets was determined to be 0.82. For

ethylene jets, the average correlation coefficients were very similar. This result defends the data illustrating that the dilution of ethylene with nitrogen or argon will give similar liftoff heights for the same inert diluent mole fraction. The average correlation coefficient for nitrogen diluted ethylene jets was determined to be 0.79, while the constant for argon diluted ethylene jets was determined to be 0.77.

These correlations can be used with either nitrogen or argon diluted methane/ethylene turbulent flames. Therefore, the new non-dimensional formulation for the modified liftoff scaling is given below

$$\frac{x_{l,y\%}}{x_{l,0\%}} \cong \left(\frac{1}{C_H}\right) \frac{\left(u_0 \rho_0^{\frac{1}{2}} \frac{1}{S_{u,m}^2}\right)_{y\%}}{\left(u_0 \rho_0^{\frac{1}{2}} \frac{1}{S_{u,m}^2}\right)_{0\%}} \tag{6}$$

This analysis of combining the two similar equations to determine the relationship with various levels of dilution is similar to that of Tieszan et al [54]. The method given by Tieszan et al., however, accounts for average turbulent jet flame speeds. The results presented exceed the limitation for the Reynolds Number (>3,200) and, therefore, that formulation cannot be used [54]. Figures 3.8 and 3.9 give graphical comparisons of the experimental liftoff heights and the scaled non-dimensional liftoff prediction seen above in Equation (6) for both methane and ethylene, respectively [35]. The correlation constant for methane, in both diluent cases, has a greater effect on the experimental data, and thus forces the data to become more compact in Figure 3.8.

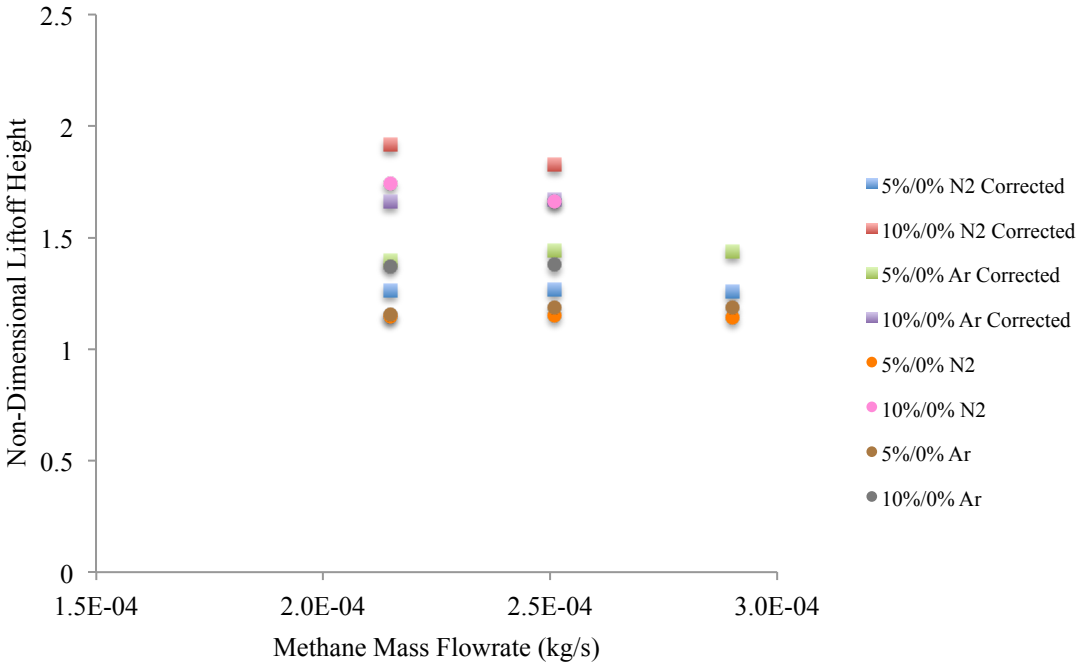

Figure 3.8: Non-Dimensional Corrected Methane Liftoff Height Values Compared to Experimental Values

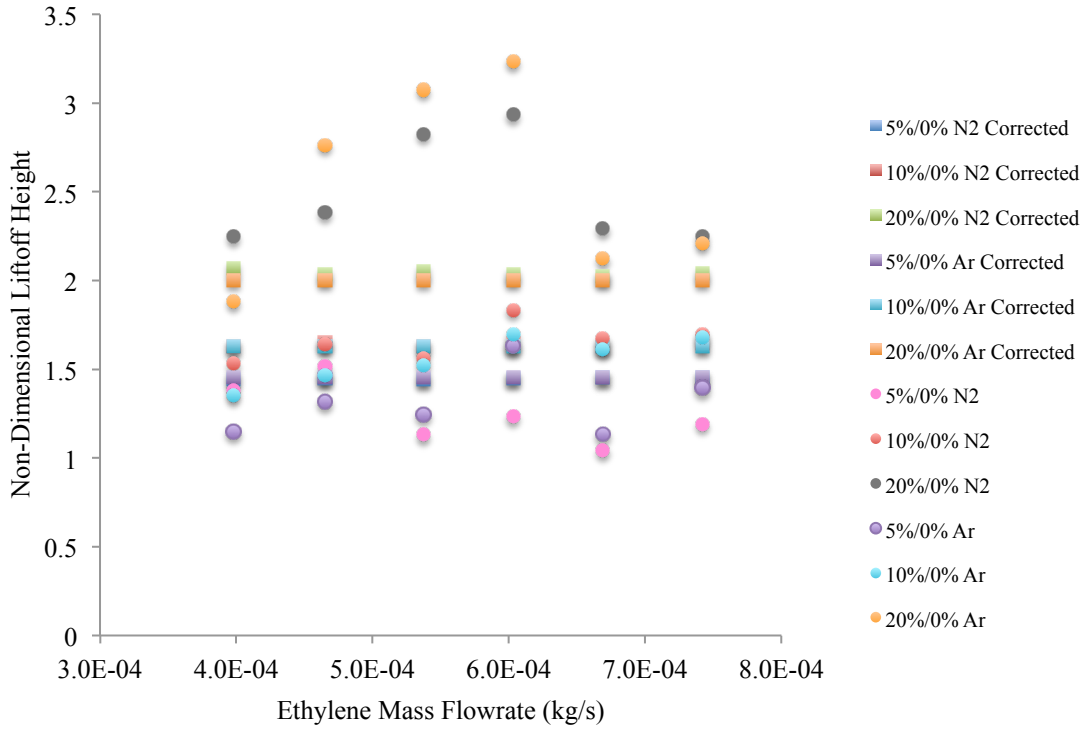

Figure 3.9: Non-Dimensional Corrected Ethylene Liftoff Height Values Compared to Experimental Values

For the ethylene plot, seen in Figure 3.9, it is established that the data undergoes minor modifications due to the more stable behavior of ethylene flames. This approximation method for non-dimensional flame liftoff height is valid over an average of liftoff heights that can be experimentally determined for various fuels. The correlation constant is related to the upper and lower flammability limits of the fuel being used. Thus, the higher the lower flammability limit and the lower the lower the upper flammability limit for the fuel being considered, the more the correlation constant should fluctuate between diluents. This fluctuation is attributed to the sensitivity of the pure fuel to the diluent being investigated.

This sensitivity can be linked to the flammability limits of both methane and ethylene. Therefore, it can be concluded that methane is more sensitive to dilution than ethylene due to its much narrower flammability region, which leads to its correlation coefficient being much more unstable between fuels and higher in average value than that of ethylene. The physical significance of the non-dimensional correlation constant described is the relation to the flammability region, as well as the flame speed of the pure fuel being examined. The lower constant determined (for ethylene) assist in describing the fewer fluctuations that are present for ethylene jets. However, the larger constant determined for methane corresponds with the instabilities that are present in methane jets.

3.6 Conclusions

The various stabilization and blowout trends of methane and ethylene jet flames diluted with diatomic nitrogen and argon have been determined. Observing these methods and analyzing their significance in comparison to theoretical results, several conclusions can be made about the affects of dilution on methane and ethylene The remarks addressing the sensitivity of the fuels to inert gases, stabilization patterns while diluted, influences on flame luminosity and soot incandescence, and non-dimensional trends with regards to flame liftoff heights are as follows:

1. It has been determined that methane is much more sensitive to inert dilution than ethylene. This sensitivity is attributed to the flammability limit variation between the two fuels, as the lower flammability region for ethylene is nearly twice that of methane. Thus, methane jets progress across the three stages of flame propagation

much more rapidly than ethylene jets. In addition, these instabilities can be attributed to the much higher flame speed of ethylene in comparison to methane [53].

2. For ethylene, the liftoff height/flame behavior is less a function of the type of diluent being used, but, instead, a strong function of the mole fraction percentage being added to the fuel. However, for methane this is not the case. The methane flame liftoff height proved to be a function of both the diluent mole fraction percentage and the type of diluent added.
3. The luminosity of the two flames was greatly affected as the mole fraction percentage of the diluents increased. As diluent levels increased it was observed that the soot radiation was steadily decreased (especially near the flame base), and the level of blue flame luminosity appeared at the flame base with dilution, indicating the position of the flame leading edge.
4. Utilizing the flame liftoff scaling formulation to predict flame liftoff heights, the non-dimensional analysis performed demonstrated the greater sensitivity of methane to the diluents over ethylene. A correlation constant was incorporated into the non-dimensional flame liftoff analysis to determine if the trends are offset by certain scaling values. It was determined that the two correlation constants for ethylene were relatively similar (which is due to the lack of dependence on diluent type for ethylene), while for methane the values varied. Plotting the results of integrating these correlation constants into the modified non-dimensional flame liftoff scaling resulted

in the data from the theoretical non-dimensional calculations being shifted to closely match that of the non-dimensional measured values [35].

CHAPTER 4: EFFECTS OF ELECTRIC FIELDS ON STABILIZED, LIFTED PROPANE FLAMES

Excerpts from: Andrew Hutchins, William Reach, James Kribs, and Kevin Lyons, Effects of Electric Fields on Stabilized, Lifted Propane Flames, ASME J. Energy Resour. Technol. (UNDER REVIEW), 2014

4.1 Abstract

The effects that various charged electrodes, and associated electric fields, have on turbulent, lifted propane flames have been investigated. Electrode polarity and primary electrode location with various flame field locations (near, mid, far) were varied, resulting in a variety of flame behavior. Results show that the body force resultant from the bulk flow of formed ions, from a positively charged fuel nozzle and grounded ring electrode, will increase liftoff height and, eventually, cause blowout. However, for the opposite polarity (positively charged ring electrode and grounded fuel nozzle) the flame progresses toward reattachment with increasing potentials. Observing the narrow window of flame blowout or reattachment (varying with polarity), it was observed that the lifted flame height fluctuations were increased with the presence of the grounded ring electrode, but reduced when the polarity was shifted to positive configuration (positively charged primary electrode). Flame hysteresis was observed when the ring electrode was positively charged and it was found that the hysteresis regime increased when the potential of the ring electrode was increased. While the ring electrode was positively charged, a distinct hole was observed in the center of the flame.

Several images are presented that show these flame holes that are present only when the electrodes are charged.

4.2 Experimental Setup

The flames observed were partially premixed, and the fuel used was propane (CP Grade, 99.0% Pure). The fuel nozzle had an inner diameter of 0.56 millimeters, and the length to diameter ratio was much greater than ten to ensure that the flow was fully developed. The volumetric flow rate of the propane gas was measured using a King Flowmeter that ranges from 0.050-0.40 standard cubic feet per hour (scfh). Observed jet velocities at the nozzle ranged from 6.41 m/s to 13.15 m/s with Reynolds Numbers varying from approximately 430 to 920. The fuel line flow was controlled using a MicroLine UHP Gas Pane regulator controller. An illustration of the described setup is given in Figure 4.1.

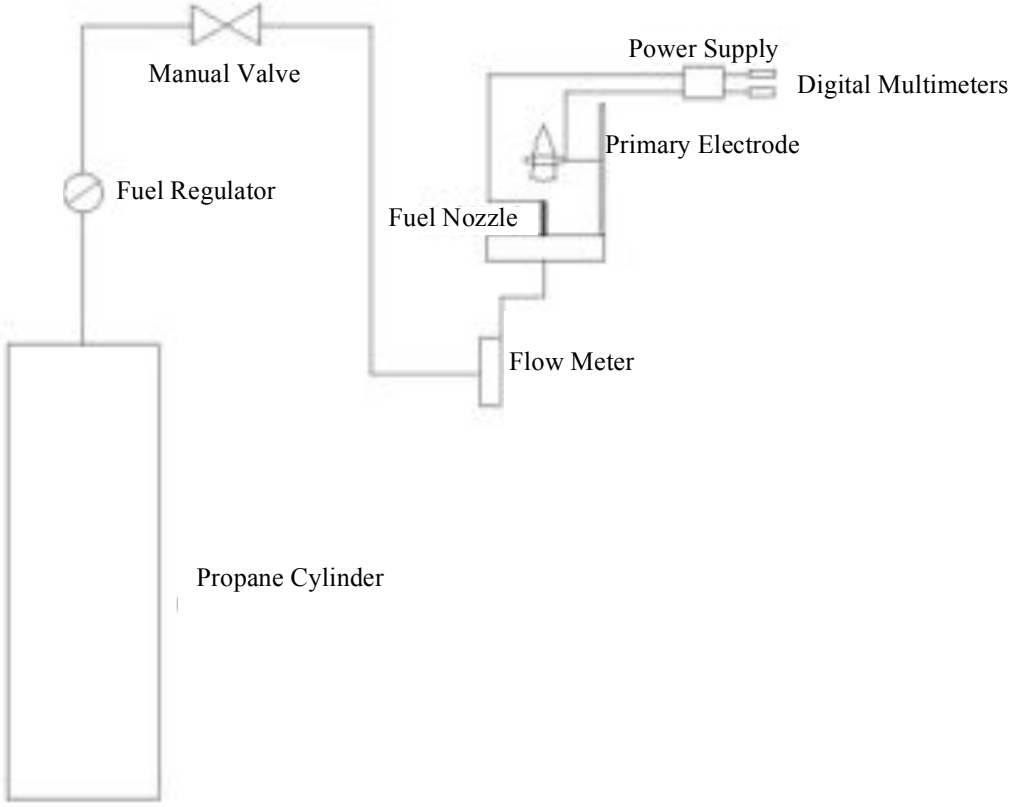

Figure 4.1: Experimental Apparatus for Electric Field Studies

The voltage applied to the ring electrode was from an Acopian Positive High Voltage Power Supply (PO30HP2). This voltage was measured using two Agilient Technologies U3401A Multimeters. Two electrodes were present in this study. The ring around the flame (with two protruding needles) was the primary electrode, and the fuel nozzle was the secondary electrode. The primary electrode consisted of a copper wire ring with two needles protruding toward the center of the axial center of the flame, as seen in Figure 4.2.

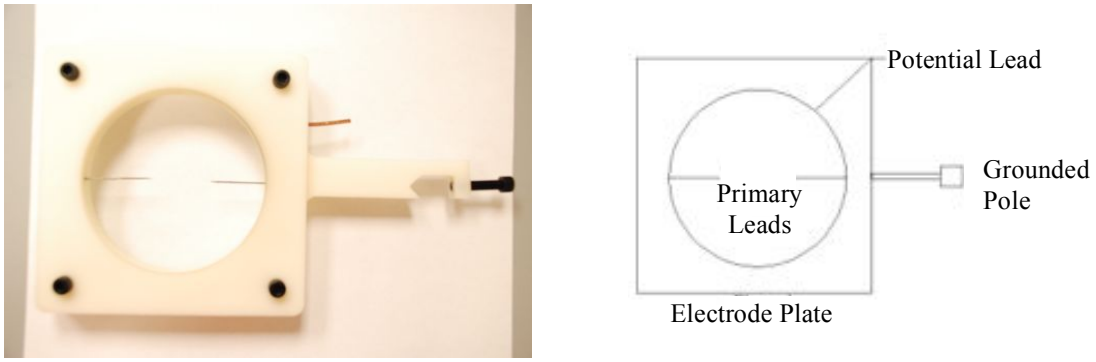

Figure 4.2: Top View of the Primary Electrode Used in all Configurations

Two scenarios were investigated with either the primary or secondary electrode being positively charged. Positive configuration refers to the primary electrode (ring with two protruding needles) being positively charged, while the secondary electrode (fuel nozzle) is grounded. Grounded configuration is the opposite polarity, with the primary electrode being grounded and the secondary electrode being positively charged. Along with varying polarities (configurations), the location of the primary electrode was varied with respect to the location of the flame. Three different ring locations were investigated: (1) The primary electrode was located at the flame base (lowest level of flame luminosity). This location varied with jet velocity due to varying flame liftoff heights. (2) The primary electrode was moved 2 inches downstream from the location in (1) for each of the varying jet velocities. (3) The primary electrode was moved 2 inches downstream from the location in (2) for each of the varying jet velocities. The total span of the flame was approximately 5 inches for all of the trials observed, thus the primary electrode was always surrounding the flame. Figure 4.3 shows how the primary electrode location varies with the different scenarios described.

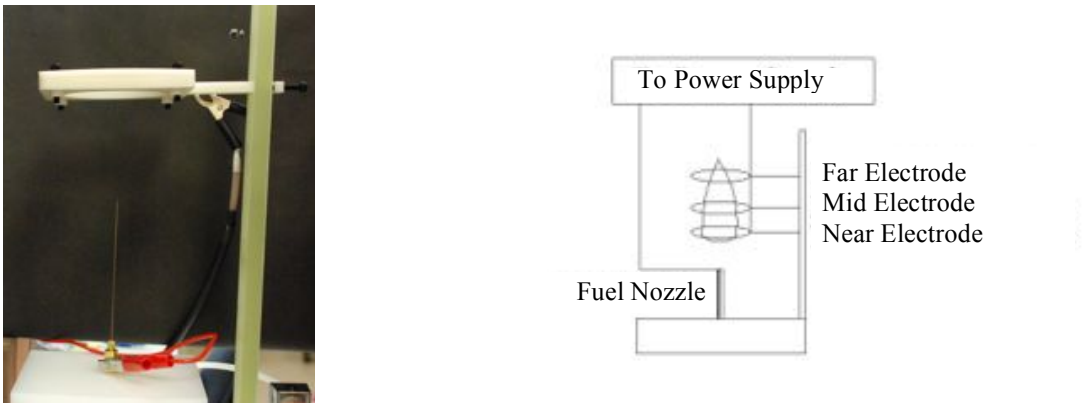

Figure 4.3: Zoomed-in on Flame Location with Varying Location of the Primary Electrode

All images were taken using a Nikon D80 Digital SLR Camera equipped with an 18-105 millimeter Nikkor Lens. Each image was taken at a distance of 34 inches from the fuel nozzle (secondary electrode) and set to a focal length of 24 millimeters. Images were analyzed on Adobe Photoshop© to ensure accuracy in lifted flame height measurements. This flame height was measured from the exit of the fuel nozzle to the lowest radial point of flame luminosity. Data recorded that exhibited flame blowout/reattachment were noted.

4.3 Results and Discussion

4.3.1 Lifted Flame Blowout/Reattachment

Flame liftoff heights, voltage potentials, and fuel jet velocities were measured and recorded for propane flames being applied to the apparatus described in Figure 4.1. The voltage was initially at 0 V (control) and was increased by 1,000 V until either flame blowout or reattachment was reached. Three propane jet velocities were used (8.02 m/s, 9.62 m/s, and 11.23 m/s) to determine if jet velocity variances magnified the influence that the electric field

had on the flame. For each of these jet velocities, the flame was lifted (partially premixed) and the near-field secondary electrode was placed at the leading edge of the reaction zone. Reynolds numbers for turbulence were much smaller than traditional turbulent values due to the micro-nozzle used in the setup (varied from 500 to 800). However, even at a Reynolds number of 550 a lifted turbulent flame was produced for a nozzle with a diameter of 0.56 millimeters.

The results of the cases consisting of the grounded configuration are given in Figure 4.4. In observing Figure 4.4, it can be seen that trends are similar across all cases in that for grounded configuration the flame is lifted at a stable height, correlated to a certain fuel jet velocity. When the electric field is applied to the flame, the liftoff heights are initially decreased until a terminal voltage is reached in which the flame trends toward blowout, while keeping the jet velocity constant. For all cases above 4 kV the affects are sporadic because of secondary ionization occurring.

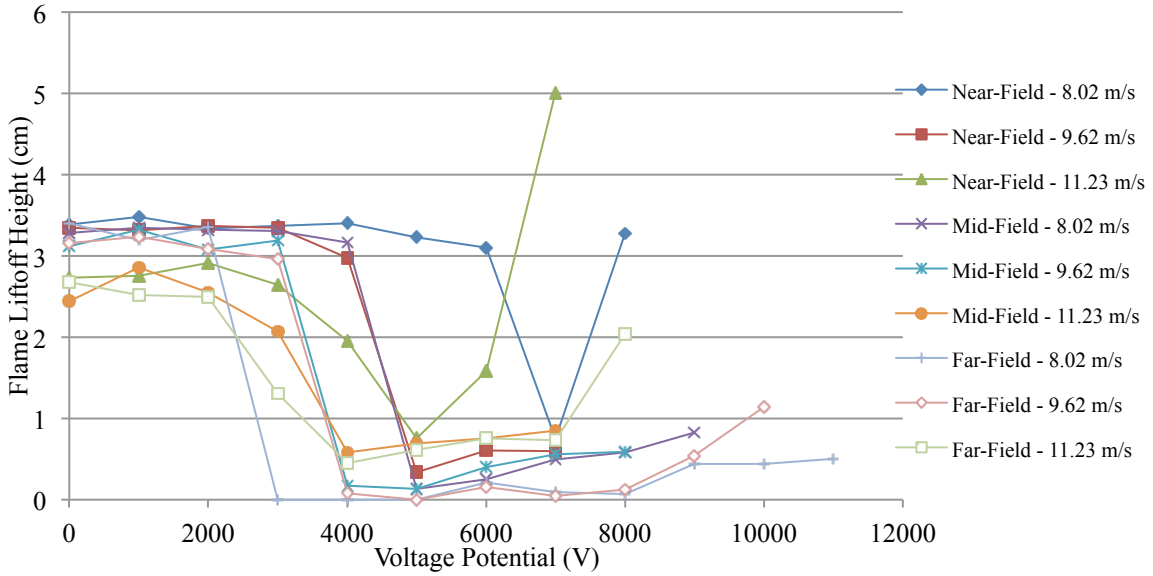

Figure 4.4: Propane Flame Liftoff Heights Under the Presence of a Charged Electrode in Grounded Configuration

Unlike the trend toward blowout that was observed in the grounded configuration cases, the tendency of the flame in the positive configuration was to reattach to the fuel nozzle at a reattachment voltage. After reattachment, the flame remained attached even as the voltage was increased past the initial reattachment voltage. Figure 4.5 gives the plot of the data described above.

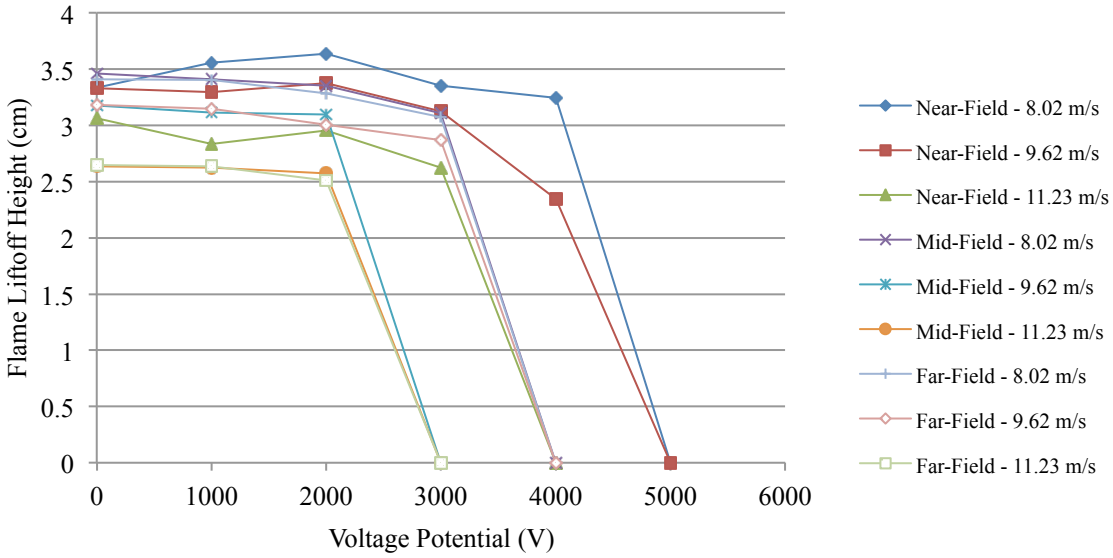

Figure 4.5: Propane Flame Liftoff Heights/Reattachment Voltages Under the Presence of a Charged Electrode in Positive Configuration

In comparing Figures 4.4 and 4.5, rapid progressions toward either blowout or reattachment is witnessed, depending on the polarity. To better observe the flame progressions as the potentials reached terminal or reattachment voltage, the step in which the voltage was increased was decreased to 100 V. By decreasing the voltage step to 100 V a better observation of flame extinction was observed. Figure 4.6 gives the three plots ((a) near, (b) mid, and (c) far-field) that illustrate the flame liftoff heights as the voltage nears its terminal value for grounded configuration. Within this region of terminal voltage, flame instabilities increase due to blowout being approached. Even with the incremental voltage increases, the flame still experienced rapid progressions toward blowout.

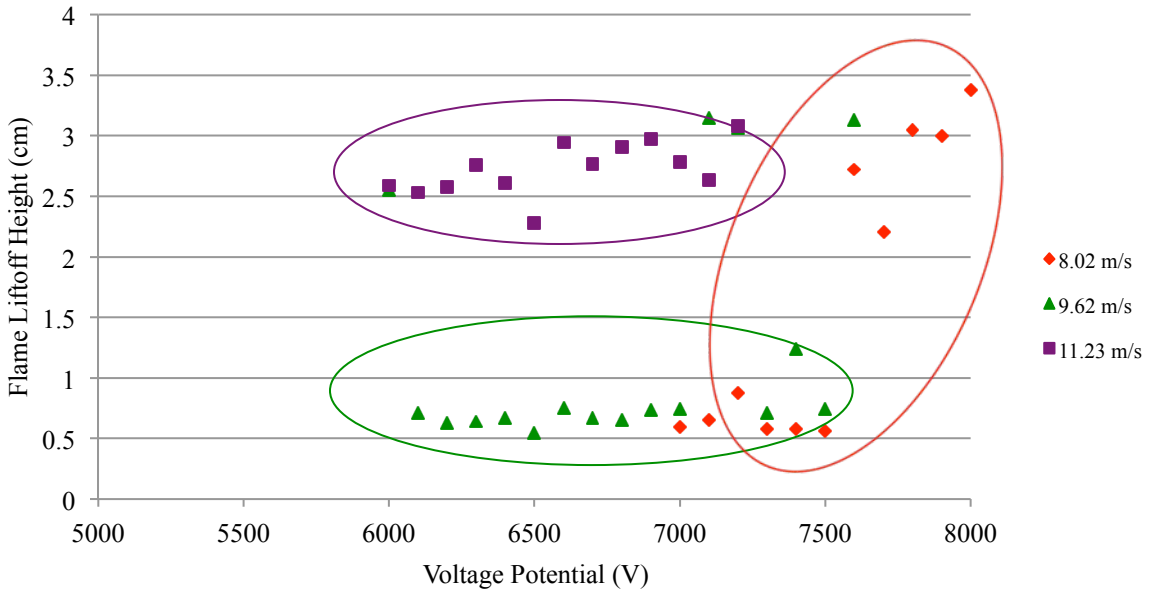

Figure 4.6(a): Near-Field Primary Electrode with 100 V Step Increases (Grounded Configuration)

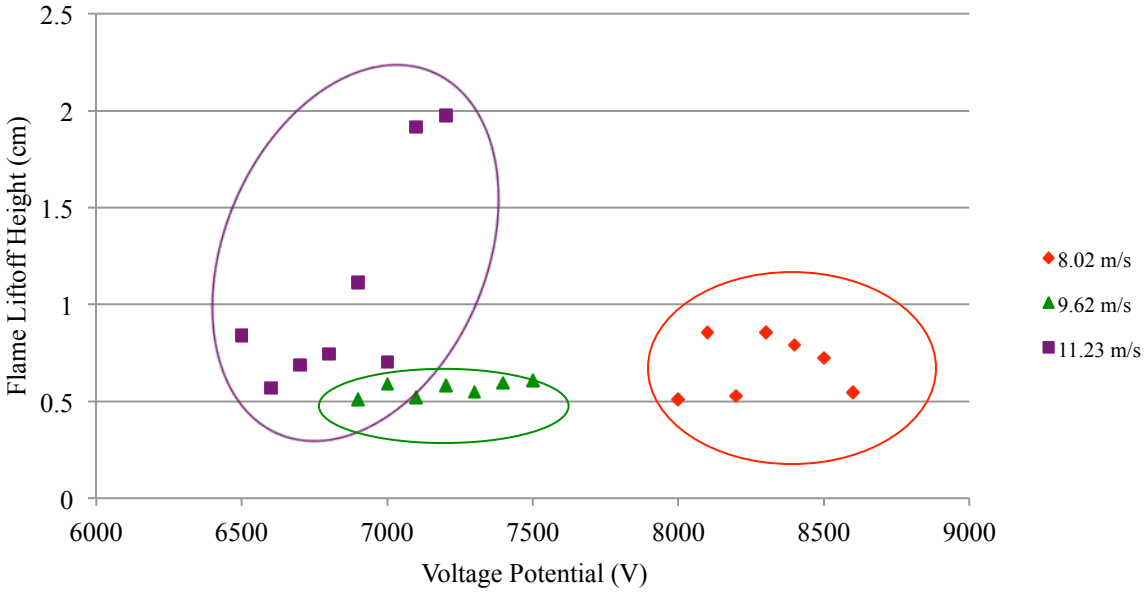

Figure 4.6(b): Mid-Field Primary Electrode with 100 V Step Increases (Grounded Configuration)

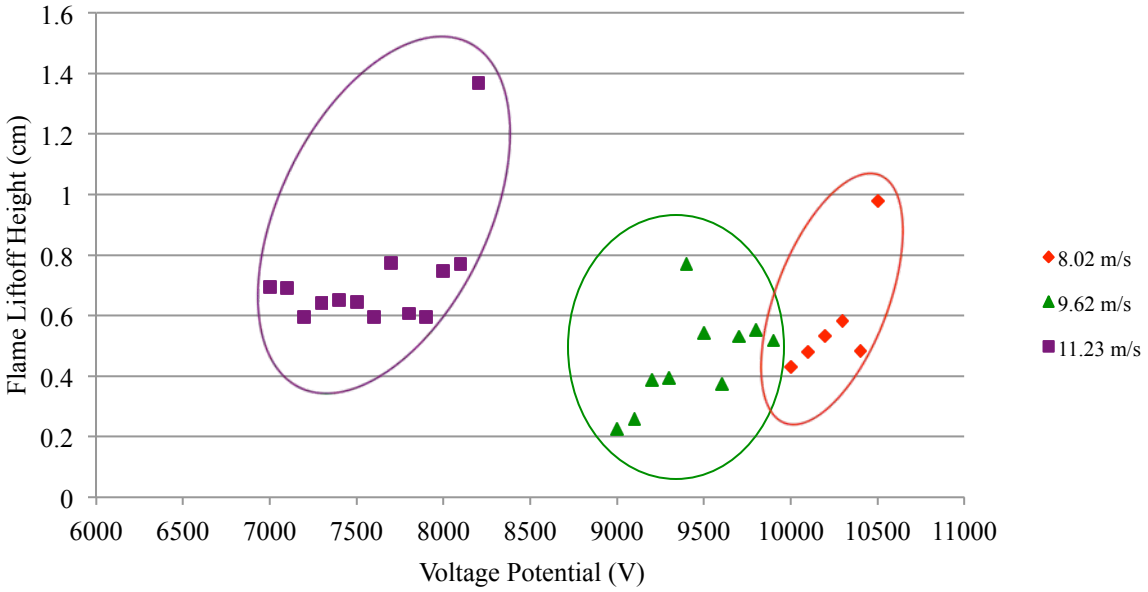

Figure 4.6(c): Far-Field Primary Electrode with 100 V Step Increases (Grounded Configuration)

Additionally, Figure 4.7(a)-(c) illustrates similar focused views for 100 V step increases for the flame under the positive configuration electric field. In the narrow reattachment voltage window, the flame lifted height fluctuations are decreased as the flame approaches nozzle reattachment. Shown in the three plots in Figure 4.7 is a relatively insensitivity to applied voltage until the reattachment voltage is abruptly reached.

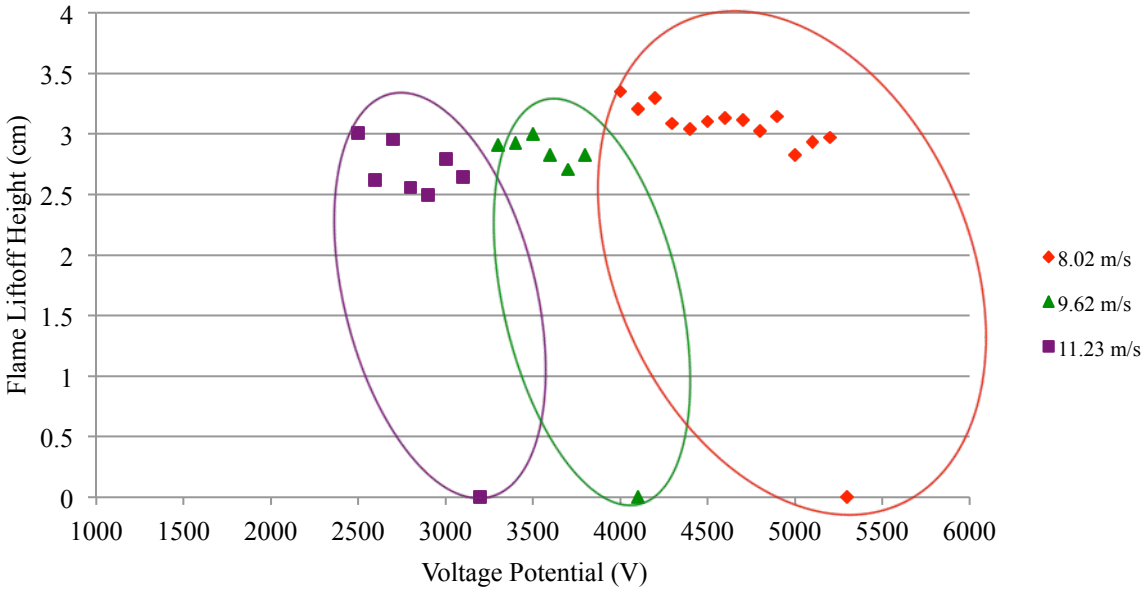

Figure 4.7(a): Near-Field Primary Electrode with 100 V Step Increases (Positive Configuration)

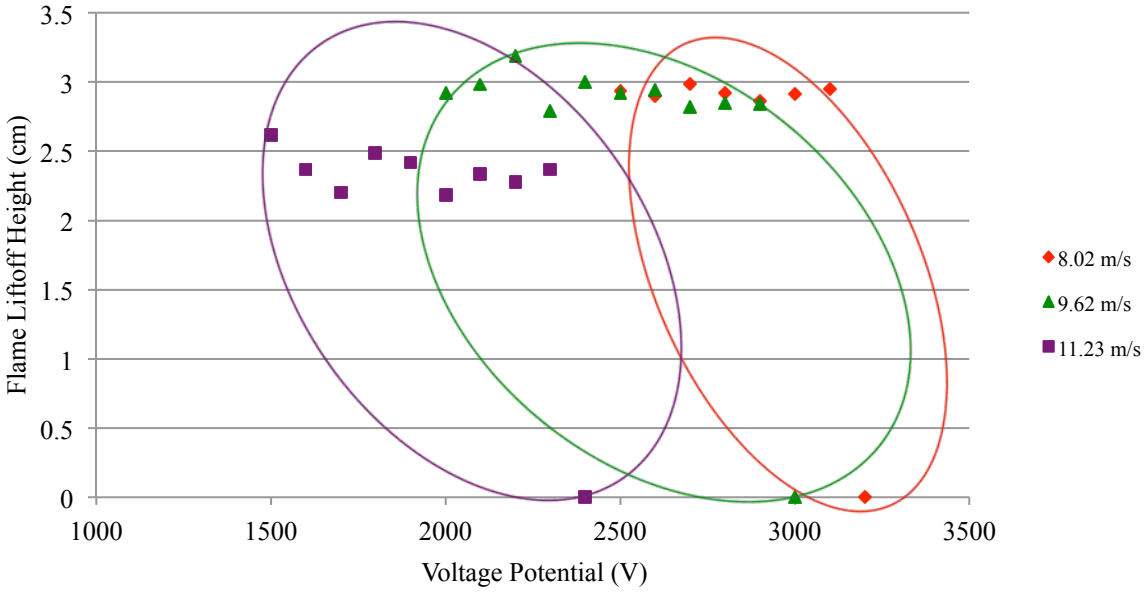

Figure 4.7(b): Mid-Field Primary Electrode with 100 V Step Increases (Positive Configuration)

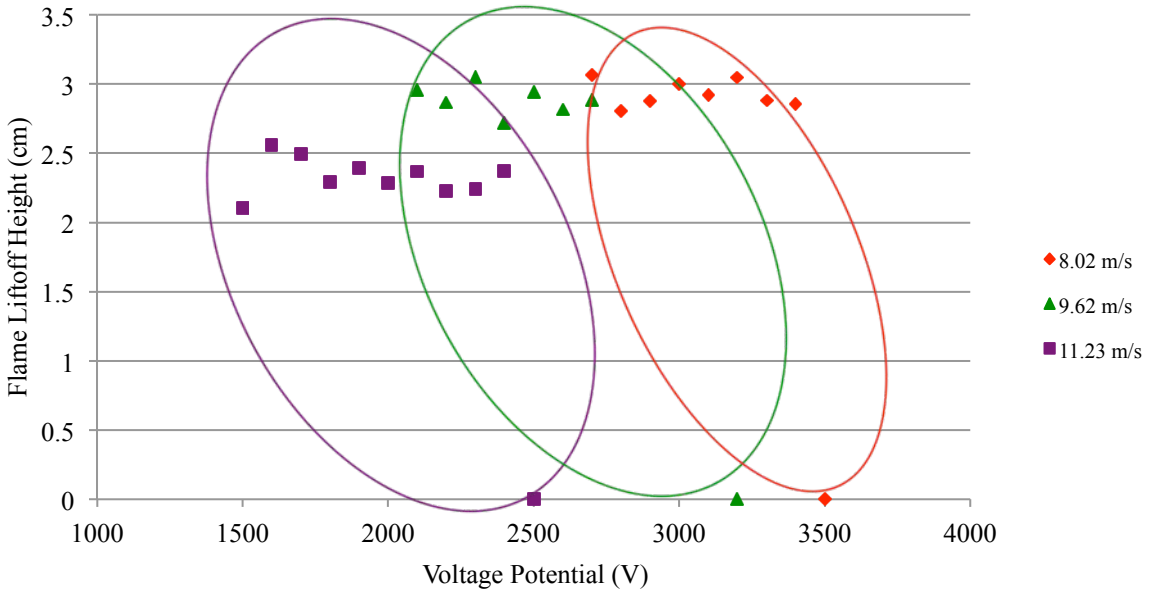

Figure 4.7(c): Far-Field Primary Electrode with 100 V Step Increases (Positive Configuration)

4.3.2 Influences on Flame Hysteresis

Studies involving flame hysteresis observations have been investigated for large-scale burners with various external influences [2,9,37]. These studies involve swirling and ambient coflow; however, the presence of a high-potential electric field has not yet been investigated when considering flame hysteresis. Typically, the flame reattachment region is dominated by the difference in the jet mixing and flame structure [1]; however, these factors are altered when an electric field is applied to the flame medium. To better investigate the impact of the field on flame hysteresis, two scenarios were studied by using the positive configuration with both cases keeping the primary electrode in the mid-field of the flame. The first case applied a certain potential (0 – 1,500 V) from flame attachment through liftoff to a maximum height,

and continued applying the voltage through flame reattachment, while altering the jet velocity at incremental values. A 0 V control test established a baseline to illustrate the standard reattachment tendency for a propane flame using the 0.56 millimeter nozzle (Figure 4.8(a)). The next cases consisted of applying 500, 1,000, and 1,500 V from liftoff through reattachment (Figure 4.8(b)-(d)). An increased difference between liftoff and reattachment velocities for increasing potentials is given in these four plots in Figure 4.8.

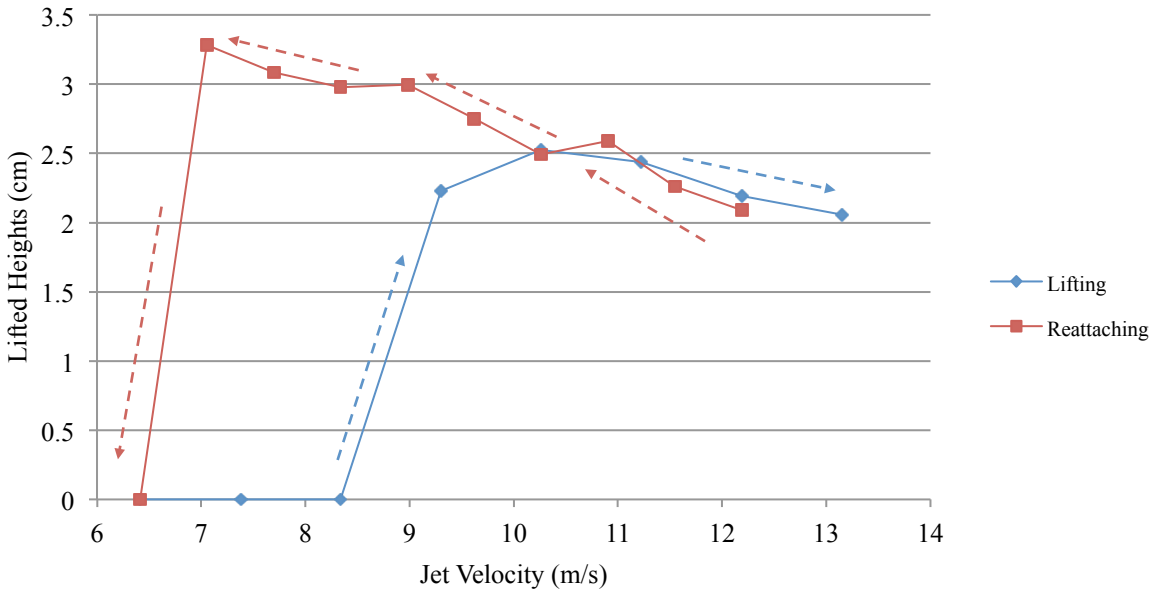

Figure 4.8(a): Hysteresis Regime for Positive Configuration with 0 V Potential

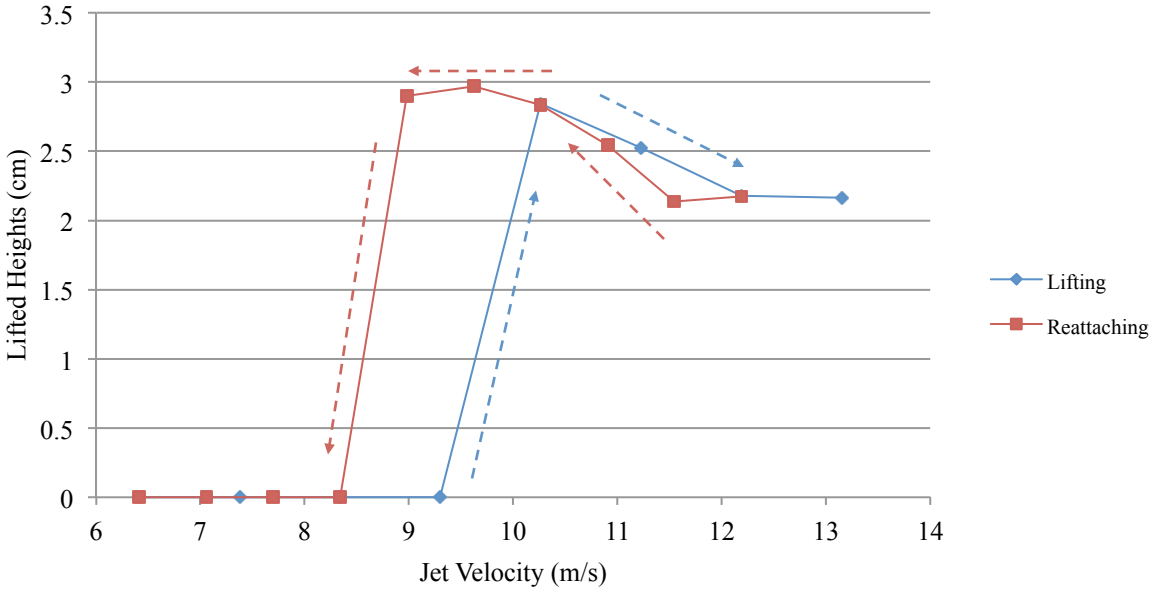

Figure 4.8(b): Hysteresis Regime for Positive Configuration with 500 V Potential

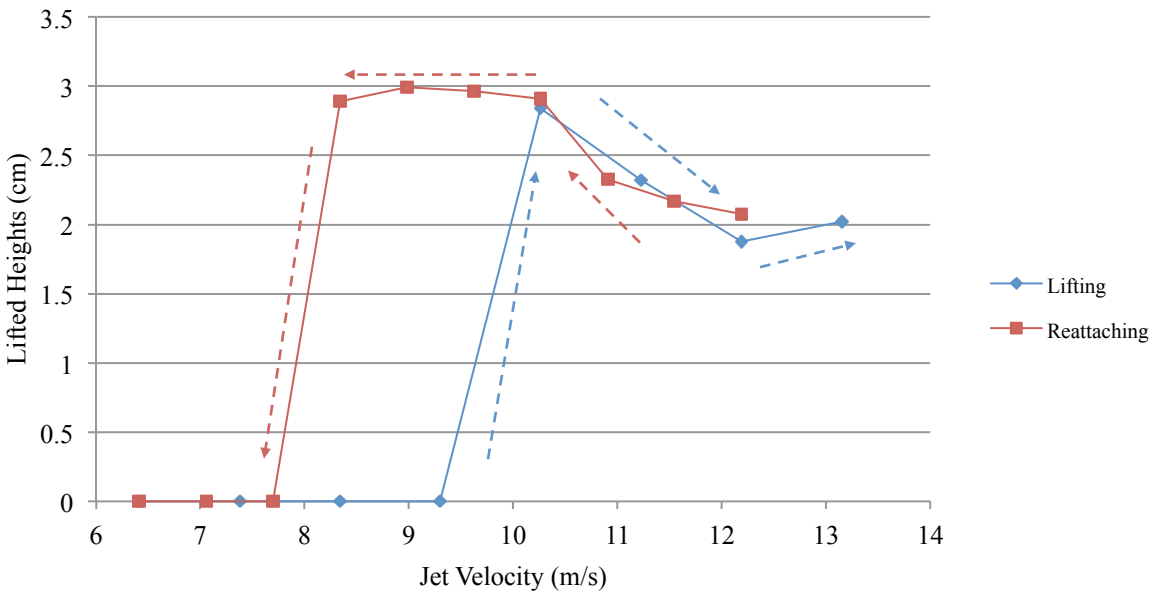

Figure 4.8(c): Hysteresis Regime for Positive Configuration with 1,000 V Potential

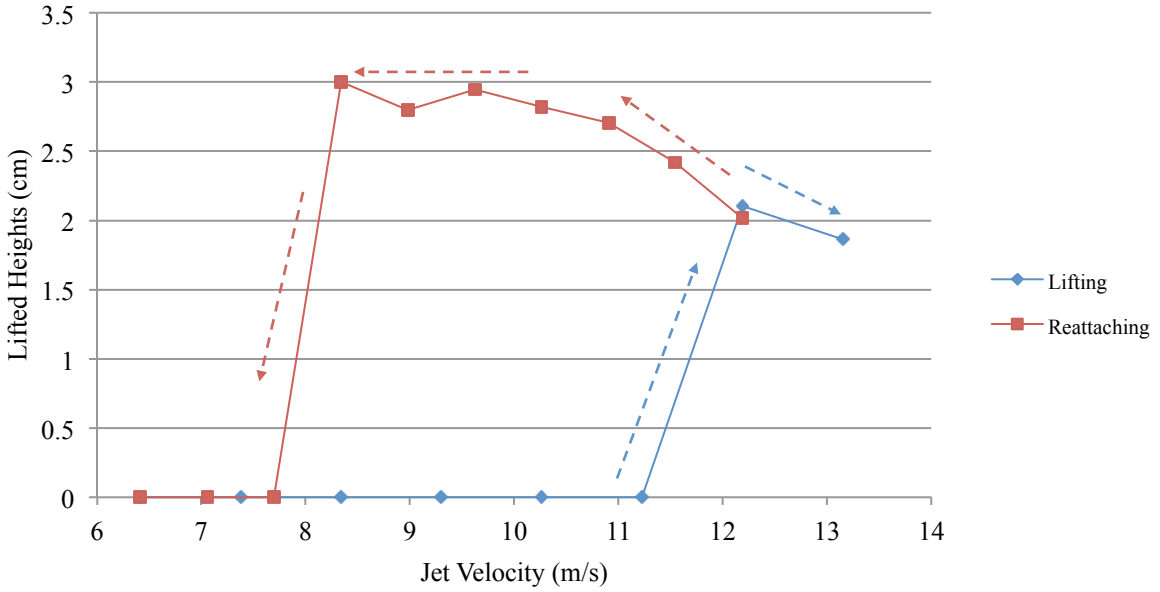

Figure 4.8(d): Hysteresis Regime for Positive Configuration with 1,500 V Potential

A second scenario was examined that altered when the electric potential was applied to the flame medium. For this test, the flame had no potential applied during liftoff, and a conventional flame progression toward a maximum jet velocity was observed (since no field is applied during liftoff). When the maximum jet velocity (13.15 m/s) was reached, the electric potential was activated to the flame medium. This set-up allowed for a higher potential to be applied to the flame (up to 2,500 V) without the flame immediately reattaching to the nozzle as illustrated in Figure 4.9. This finding has direct implication in conserving fuel in stabilizing jet flames, while underscoring the optimization of flame control and the importance of timing the initial application of the electric field.

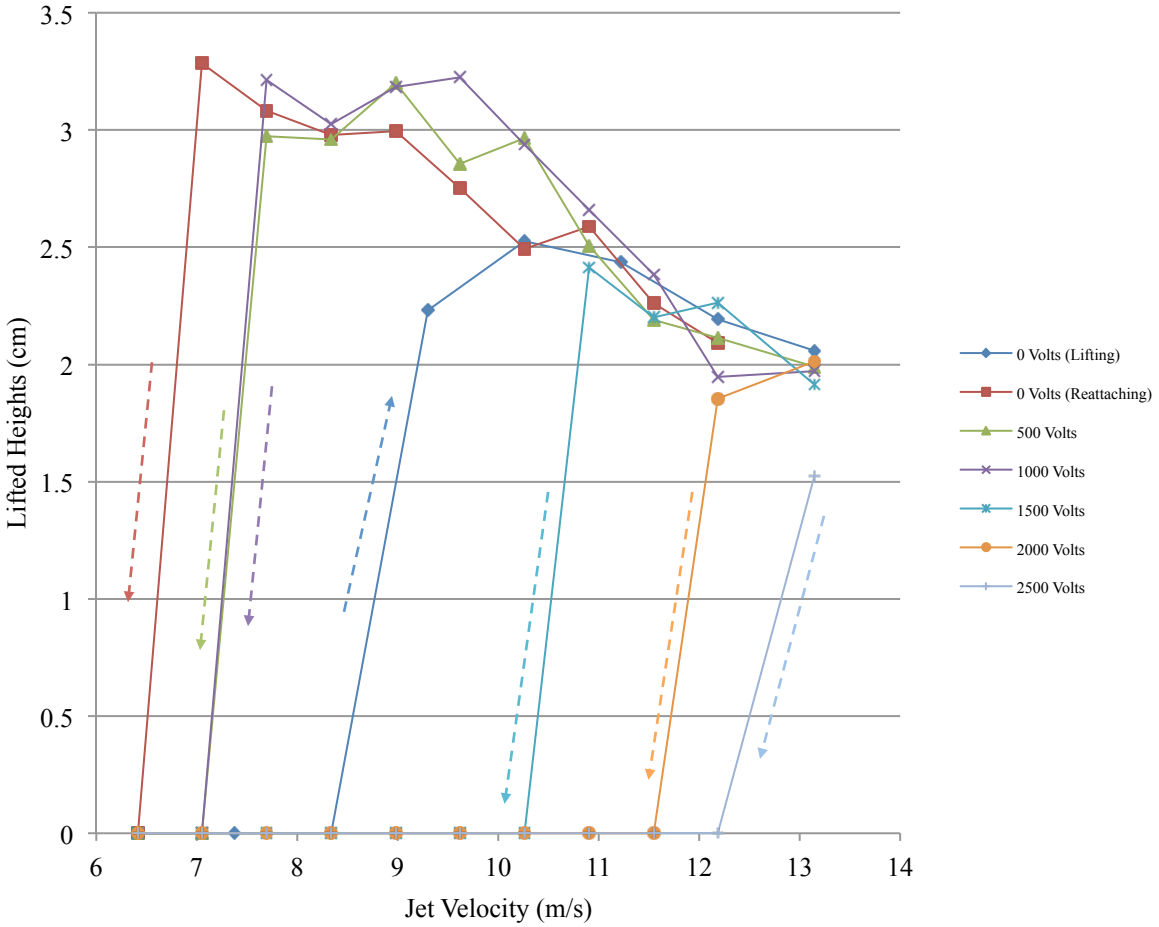

Figure 4.9: Hysteresis Regimes when Positive Configuration Potential is Applied Only During Reattachment

4.3.3 Electric Field Effect on Flame Stability

Observing the figures described previously, it is seen that flame behavior varies greatly depending on the polarity of the primary and secondary electrodes. These variations in flame stability are attributed to the bulk flow of the ions created from the respective electrodes. This bulk flow attributes to a body force that is generated on the flame from the motion of these ions. This body force is given as

$$F = Ee(n_+ - n_-) = neE \tag{7}$$

where n_+ and n_- are the number density of the ions present with a positive or negative charge and e is the fundamental charge of an electron. The equation is simplified because opposite polarity charges do no exist in a wide-range [55]. An alternative representation of this body force can be shown as

$$F = \frac{J}{K} = \frac{neKE}{K} \tag{8}$$

where J is the local current density [55]. This body force is what creates a phenomenon known as the "ionic wind." The ionic wind is formed from a sharp, positively charged object and a grounded electrode that is separated by a gas medium subjected to an electric field [56]. This ionic wind is also known as the "corona wind" [57] due to the corona discharge that develops at the sharp edge of the charged electrode. The body force produced by these charged particles affect the manner in which the flame stabilizes, in addition to liftoff/blowout tendencies. A representation of the bulk flow of these ions is given in Figure 4.10.

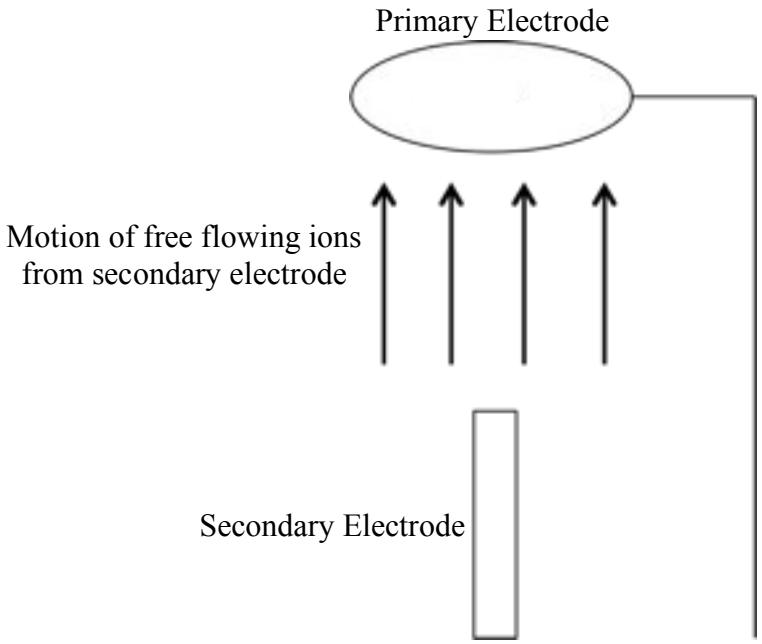

Figure 4.10: Representation of the Motion of the Bulk Flow of the Formed Ions

The body force that is directed by the bulk flow of these ions could assist in controlling whether the flame will trend toward blowout or reattachment. The direction of the ion flow is the same regardless of the polarity of the configuration due to the sharp fuel nozzle being charged. Since the primary electrode ring is not a single sharp electrode the direction is toward the ring electrode and away from the single, sharp secondary electrode. Upon observing Figure 4.10 in detail and comparing the flame behavior variance from grounded to positive configuration it is seen that the direction of the bulk ion flow is consistent for grounded configuration when the flame tends toward blowout; however, for positive configuration when the flame is moving toward the nozzle for reattachment the bulk flow direction is opposite in direction. From this observation it can be concluded that for this

set-up, the ions produced from the charged electrodes have little control in the direction that the leading edge of the flame moves.

To better observe Figures 4.4 and 4.5, two normalized plots are given in Figures 4.11 and 4.12. In comparing Figure 4.4 to Figure 4.11, not much discrepancy is present when the lifted height of the flame is normalized. However, the magnitude of how much the flame heights fluctuate as the potential is increased is clearly shown when the heights are non-dimensionalized. A similar comparison can be made when observing Figures 4.5 and 4.12.

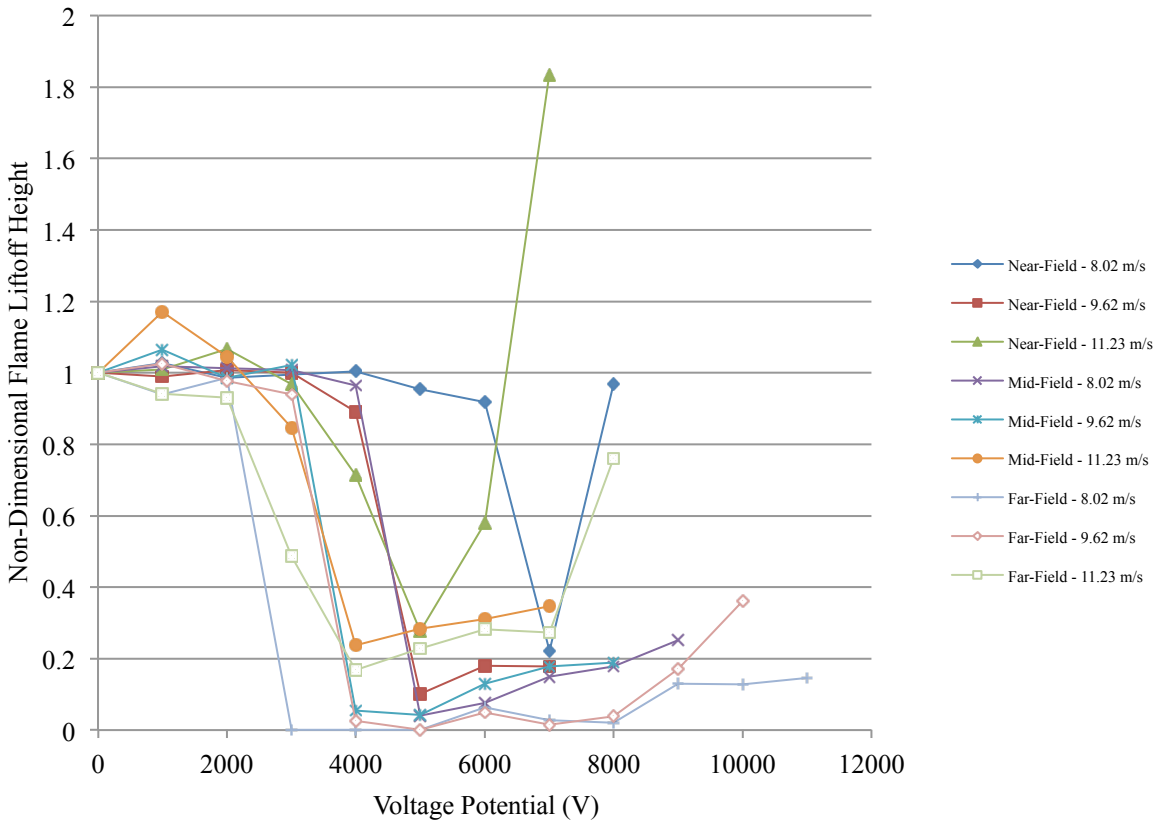

Figure 4.11: Normalized Liftoff Heights for the Grounded Configuration

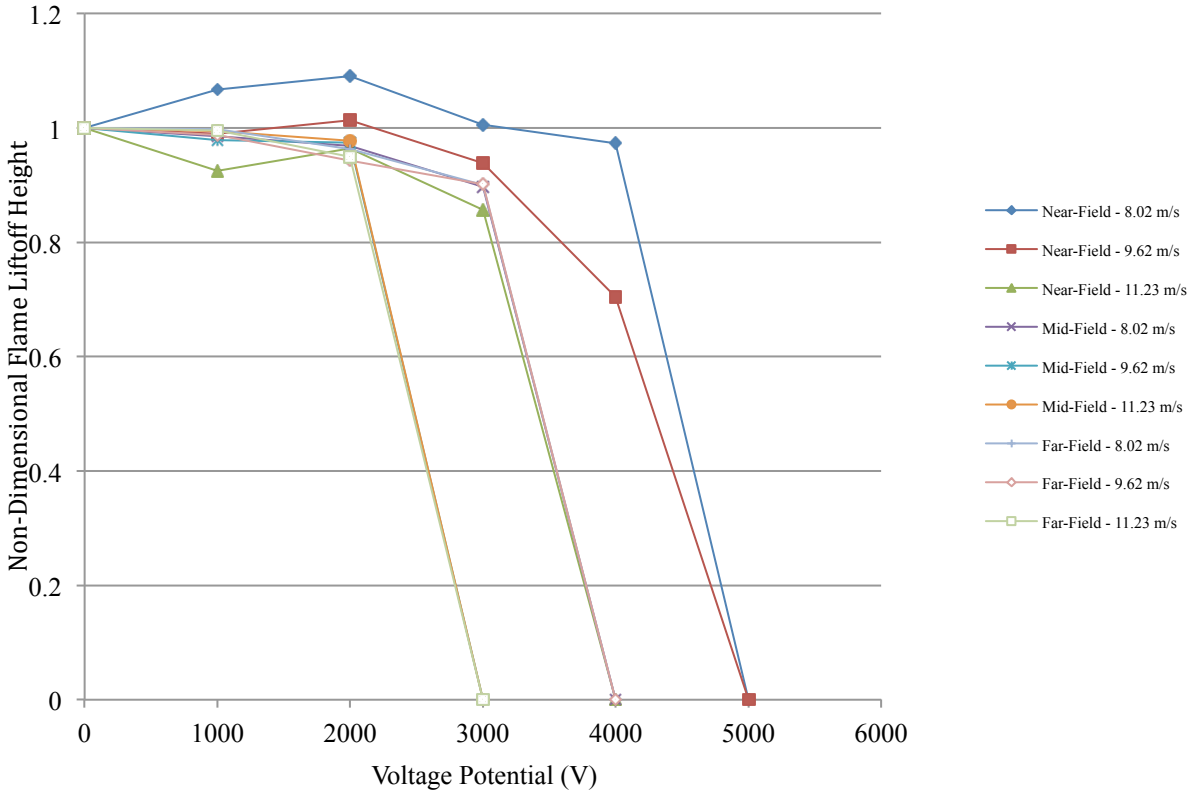

Figure 4.12: Normalized Liftoff Heights for the Positive Configuration

These two normalized plots illustrate the discussed observations in such a way that the overall influenced of the electric field on the flame stability and control are easier to see, especially when comparing across various jet velocities.

The discussions provided on flame stability shed light into the possibility of better combustion control with the application of a high-potential electric field being present around a flame. Benefits Behind using an electric field to control flame behavior are as follows: lower fuel consumption, thermal stress mediation on the fuel nozzle, better control of flame

liftoff heights, limiting flame blowout, and overall flame stability. These benefits are sought after in industrial applications, especially with the increasing need for fuel conservation.

4.3.4 Inducement of Reaction Zone Discontinuity

Empirical studies by Nayagnam et al. [58] express the possibilities that “flame holes” can be present in diffusion flames. This study states that the size of these possible “flame holes” is directly related to the Damkohler Number and states that the presence is theoretically possible. Upon closer observations of several of the images taken from the hysteresis results stated above, it was observed that large flame discontinuities were present in several images. This evidence that flame holes are present has not been defended experimentally due to the rapid fluctuations in temperature and lateral gradients that occur in turbulent flames. However, in Figure 4.13 three images are presented that clearly show a discontinuity between the saturated soot flame tip and another “soot pocket” that is separate from the flame itself. The evidence shown in Figure 4.13 is when the electric field is applied to the flame in positive configuration and with varying jet velocities. Thus, it is possible that this type of phenomenon is occurring at a much smaller scale within flames that are not under the presence of an electric field, but the application of these high-potentials heavily influences this discontinuity and exaggerates the size of the flame hole. This split reaction zone is induced by the activation of the electric field and has the potential to be useful in overall combustion control.

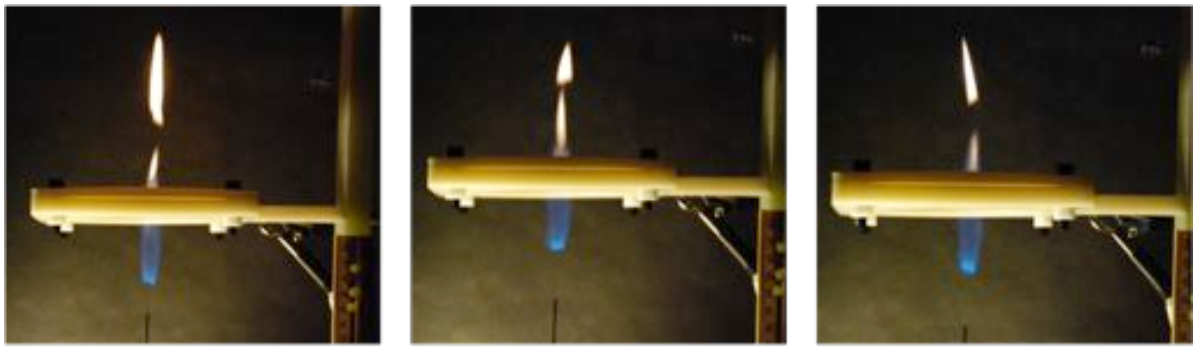

Figure 4.13: Various Images of Flame Discontinuity Induced by the Electric Field

4.4 Conclusions

The effects of a charged electrode at various locations of a lifted propane flame have been investigated. The results that have been presented verify that an electric field presence greatly affects the way the lifted flame stabilizes. The novel findings that have been reported are:

1. Under the presence of an electric field, it has been demonstrated that varying the polarity of the field, as well as the location of the primary electrode, can control propane flame stabilization. A grounded primary electrode (ring) and positively charged secondary electrode (fuel nozzle) will push the flame tendency toward blowout, while a positively charged primary electrode (ring) and grounded electrode (fuel nozzle) promotes stable and continuous reattachment of the flame to the fuel

nozzle. These two phenomena are attributed to the varying pools of ions that the two fields create within the medium (flame).

2. Varying the location of the electrode ring with respect to different positions within the lifted propane flame proved to have varying influences depending on polarity. For grounded configuration (grounded primary electrode and positively charged secondary electrode), the flame was able to stabilize at higher voltage potentials when the field was located in the far-field (up to ~10,000 V). However, for positive configuration, the location of the electrode had little influence on the reattachment voltage of the flame. Instead, the fuel jet velocity was the dominant factor. At the highest jet velocity (11.23 m/s) more ions were produced around the nozzle, and thus the flame reattached at lower voltages in comparison to lower jet velocities (8.02 m/s and 9.62 m/s).
3. For both the positive and grounded electrode configurations, the lifted height of the flame experienced rapid progressions to either blowout (grounded configuration) or reattachment (positive configuration). When incremental voltage increases were observed, it was noted that when the primary electrode was grounded, the flame lifted heights were increased with incremental voltage increases. However, when the primary electrode was positively charged the liftoff height was largely insensitive to voltage, but a rapid progression to reattachment was present with the 100 V incremental increases.

4. Upon observing the reattachment regime for flames under positive configuration, it was determined that the hysteresis regime varies greatly when the flame is under the presence of an electric field. The upper region of the flame progressing toward blowout is not present, and as the jet velocity is decreased to progress toward reattachment, the flame will be lifted higher within the hysteresis regime. These hysteresis variations presented in this paper are the first to be reported in the literature and discussed with respect to the presence of an electric field.
5. While the electric field was activated, a flame discontinuity was intermittently observed downstream from the primary electrode. After the primary soot saturated region of the flame, a region of suppressed combustion was present, followed by a sooting region near the tip. This observed flame phenomena, has not been not been theoretically predicted and is reported here for the first time. This complex, transient occurrence warrants further investigation.

CHAPTER 5: SUMMARY

5.1 Concluding Remarks

Continued research in the area of turbulent flame control is a very important topic to many industrial and commercial applications. New studies shed light into methods of conserving fuel and designing more efficient burners. The three studies presented in this thesis present methods that could potentially assist in new methods of flame control. From each of these studies various conclusions were presented and several questions were answered.

In discussing the methods of flame confinement the following conclusions were drawn:

1. Methane flames stabilize at much different heights when the flame is confined from the ambient surroundings.
2. Semi-confined flames behave sporadically due to an increase in swirl at the viewing window; however, a methane flame that is fully confined lifts at similar heights to that of an unconfined methane flame.
3. Lower lifted heights were observed for the semi-confined methane flame in comparison to the fully confined and unconfined methane flames.
4. A higher jet velocity is required for both semi-confined and fully confined flames to attain initial liftoff.

The results from diluting methane and ethylene with various diluents (nitrogen and argon) uncovered both experimental and empirical results:

1. Methane flames were proven to be much more sensitive to dilution in comparison to ethylene flames, regardless of the jet velocity or the type of diluent applied.
2. Ethylene flame heights were proven to be a function of the mole fraction of the diluent used and not the type of diluent; however, for methane flames, the liftoff heights were both a function of diluent type and diluent mole fraction.
3. Flame luminosity variations were observed for both methane and ethylene flames (more obvious in ethylene flames). Soot incandescence was decreased as dilution levels increased, in particular at the flame base of the ethylene flames. Therefore, the typically soot-saturated ethylene flame presented a bluer luminescence (cleaner) at the leading edge of the flame.
4. A correlation constant was incorporated into the Broadwell scaling analysis [35] that corrected for the type of diluent used in both methane and ethylene jet flames. Ethylene correlation constants were found to be similar in magnitude; however, methane constants were greater in magnitude and varied greatly depending on diluent type. Thus, proving that methane flame lifted heights are functions of both diluent type and diluent mole fraction.

Several observations were made in applying a high-potential electric field to a lifted propane flame:

1. The behavior of a propane flame under the presence of a high-potential electric field is dependent on the polarity of the electric field. A grounded primary electrode and positively charged secondary electrode will result in progression toward flame blowout after secondary ionization. When the polarity is flipped, the propane flame progressed toward reattachment with increasing potentials.
2. While in the grounded configuration, the flame was able to stabilize at higher potentials when the primary electrode was located in the far-field. For positive configuration, the location of the primary electrode had little influence on the flame behavior. Thus, the jet velocity was the dominant factor in determining the flame lifted height in the positive configuration.
3. A rapid progression toward blowout/reattachment was observed for both polarities. When 100 V steps were used, the flame still had tendency to rapidly blowout or reattach depending on the field polarity. For grounded configuration flame heights increased with incremental voltage steps; however, for positive configuration, the flame was insensitive to incremental changes in voltage.
4. In observing the hysteresis patterns of the propane flame with the application of the electric field, it was observed that while under positive configuration the flame hysteresis regime was greatly altered. Typical hysteresis plots were not seen. Instead, the flame upper region of flame instability to blowout was not present, and the flame was lifted higher within the hysteresis regime.

5. A flame discontinuity was observed downstream from the primary electrode. After this discontinuity, a soot-saturated region was present.

5.2 Future Work

Each of the three studies described in this report warrant further investigation into novel methods of flame control. Continued research into improved methods could lead to safer working environments, fuel conservation, more efficient industrial devices (boiler, burners, etc.), and longer life spans of these devices due to reduced thermal stresses on the fuel nozzle.

More extensive studies in confined/semi-confined jets would involve a new apparatus that permit the fuel jet velocity to approach a near blowout limit. The results from this test would inform us on the magnitude of the shift in the blowout velocity that is required for methane when it is under any kind of confinement. In addition, modifying the window geometry and creating/offsetting additional windows throughout the confinement cylinder would give various swirling patterns that would encourage more mixing, in the semi-confined case. In order to determine how much turbulent mixing is being added to the combustion chamber from the open window, in the semi-confined case, two methods can be used: (1) Particle Image Velocimetry (PIV) can be used to track tracer particles that can be included in the fuel line and will give the relative instantaneous velocity profile of the coflow or (2) k-ε models can be observed in a computational modeling software to get a theoretical profile of how the mixing is being altered.

Further investigation should dilute methane and ethylene jet flames with other inert gases to determine if further correlation coefficients can be determined. The observation of the range of C_H could be tested as well for other fuels (such as propane) to determine if the coefficient indeed falls within the limits suggested. In addition to testing pure fuels with inert diluents, a further investigation should involve various fuel mixtures with inert diluent to determine fuel dominance in determining this correlation coefficient.

In observing flame behavior under the presence of a high-potential electric field, there are many more questions that still need to be addressed. Only a limited number of fuels (most commonly propane) have been experimented with when incorporating an electric field in the flame medium. Additional tests with other gaseous fuels, and eventually liquid fuels in spray flames, would enlighten us on if the trends that have been described are present for all flames. Various geometries of the primary electrode, such as more needles from the charged copper ring, are expected to give various results in flame stability.

Other studies that are of interest involve micro-size nozzles that produce micro-scale flames. These small flames have not been heavily investigated due to the difficulty of visualization and keeping the flame present in a room with any air movement. In particular, a topic that is of interest is observing lifted laminar flames that are produced from these micro-scaled nozzles. These types of flames are becoming more prevalent in the research area of micro-combustors and micro-aerial vehicles (MAVs). The benefit of observing lifted laminar flames is the ability to accurately model and predict flame behavior. Unlike turbulent flames, laminar flames can be predicted with various equations that are generated from the Navier

Stokes Equations. Incorporating the study of high-potential electric fields with these micro-flames is an area that shows promise for several new applications.

REFERENCES

[1] Gollahalli, S.R., Savas, O., Huang, R.F. and Rodriquez Azara, J.L., "Structure of Attached and Lifted Gas Jet Flames in Hysteresis Region," *Symposium (International) on Combustion*, vol. 21, pp. 1463-1471, 1988.

[2] Terry, S.D. and Lyons, K.M., "Turbulent Lifted Flames in the Hysteresis Regime and the Effects of Coflow," *ASME Journal of Energy Resources Technology*, vol. 128, pp. 319-324, 2006.

[3] Lyons, K.M., "Toward an Understanding of the Stabilization Mechanisms of Lifted Turbulent Jet Flames: Experiments," *Progress in Energy and Combustion Science*, vol. 33, no. 2, pp. 211-231, 2007.

[4] Schefer, R.W., "Stabilization of Lifted Turbulent Jet Flames," *Combustion and Flame*, vol. 99, no. 1, pp. 75-78 1994.

[5] Saeys, L.J., Zumer, M. and Dealy, J.M., "Criteria for Recirculation in Confined Jet Flames," *Combustion and Flame*, vol. 17, no. 3, pp. 367-377, 1971.

[6] Lawn, C.J., "Lifted Flames on Fuel Jets in Coflowing Air," *Progress in Energy and Combustion Science*, vol. 35, no. 1, pp. 1-30, 2009.

[7] Cha, M.S. and Chung, S.H., "Characteristics of Lifted Flames in Nonpremixed Turbulent Confined Jets," *Symposium (International) on Combustion*, vol. 26, pp. 121-128, 1996.

[8] Iyogun, C.O. and Birouk, M., "Stability of a Turbulent Jet Methane Flame Issuing from an Asymmetrical Nozzles with Sudden Expansion," *Combustion Science and Technology*, vol. 181, no. 1, pp. 1443-1463, 2009.

[9] Moore, N.J., Terry, S.D. and Lyons, K.M., "Flame Hysteresis Effects in Methane Jet flames in Air-Coflow," *ASME Journal of Energy Resources Technology*, vol. 133, no. 2, pp. 319-324, 2011.

[10] Leung, T. and Wierzba, I., "The Effect of Co-flow Stream Velocity on Turbulent Non-premixed Jet Flame Stability," *Symposium (International) on Combustion*, vol. 32, no. 2, pp. 1671-1678, 2009.

[11] Moore, N.J. and Lyons, K.M., "Leading-Edge Flame Fluctuations in Lifted Turbulent Flames," *Combustion Science Technology*, vol. 182, no. 7, pp. 777-793, 2010.

[12] Moore, N.J., McCraw, J.L. and Lyons, K.M., "Observations on Jet Flame Blowout," *International Journal of Reacting Systems*, vol. 2008, pp. 1-7, 2008.

[13] Takahashi, F., Mizomoto, M., Ikai, S. and Futaki, N., "Lifting Mechanisms of Free Jet Diffusion Flames," *Symposium (International) on Combustion*, vol. 20, no. 1, pp. 295-302, 1985.

[14] Wu, Y., Lu, Y., Al-Rahbi, I.S. and Kalghatgi, G.T., "Prediction of the Lift-off, Blow-out and Blow-off Stability Limits of Pure Hydrogen and Hydrocarbon Mixture Jet Flames," *International Journal of Hydrogen Energy*, vol. 34, pp. 5940-5945, 2009.

[15] Watson, K.A., Lyons, K.M., Donbar, J.M. and Carter, C.D., "Simultaneous Rayleigh Imaging and CH-PLIF Measurements in a Lifted Jet Diffusion Flame," *Combustion and Flame*, vol. 123, no. 1-2, pp. 252-265, 2000.

[16] Watson, K.A., Lyons, K.M., "Simultaneous Two-Shot CH Planar Laser-Induced Fluorescence and Particle Image Velocimetry Measurements in Lifted CH_4/Air Diffusion Flames," *Symposium (International) on Combustion*, vol. 29, no. 2, pp. 1905-1912, 2002.

[17] Moore, N.J., Kribs, J.D. and Lyons, K.M., "Investigation of Jet-Flame Blowout with Lean-Limit Considerations," *Flow, Turbulence and Combustion*, vol. 87, no. 4, pp. 525-536, 2011.

[18] Karbasi, M. and Wierzba, I., "Prediction and Validation of Blowout Limits of Co-flowing Jet Diffusion Flames—Effect of Dilution," *ASME Journal of Energy Resources Technology*, vol. 120, no. 2, pp. 167-171, 1998.

[19] Chao, Y.C., Wu, C.Y., Lee, K.Y., Li, Y.H., Chen, R.H. and Cheng, T.S., "Effects of Dilution on Blowout Limits of Turbulent Jet Flames," *Combustion Science and Technology*, vol. 176, pp. 1735-1753, 2004.

[20] Kalghatgi, G.T., "Blow-out Stability of Gaseous Jet Diffusion Flames," *Combustion Science and Technology*, vol. 26, no. 5-6, pp. 233-239, 1981.

[21] Smooke, M.D., McEnally, C.S., Fielding, J., Long, M.B., Pfefferie, L.D., Hall, R.J. and Colket, M.B., "Investigation of the Transition from Lightly Sooting Towards Heavily Sooting Coflow Ethylene Diffusion Flames," *Combustion Theory and Modelling*, vol. 8, pp. 593-606, 2004.

[22] Lee, S.M., Park, C.S., Cha, M.S. and Chung, S.H., "Effect of Electric Fields on the Liftoff of Nonpremixed Turbulent Jet Flames," *IEEE Transactions on Plasma Science*, vol. 33, no. 5, pp. 1703-1709, 2005.

[23] Weinberg, F.J., Carleton, F.B. and Dunn-Rankin, D., "Electric Field-Controlled Mesoscale Burners," *Combustion and Flame*, vol. 152, no. 1-2, pp. 186-193, 2008.

[24] Tret'yakov, P.K., Tupikin, A.V., Denisova, N.V., Ganeev, O.V., Zamashchikov, V.V. and Kozorezov, Y.S., "Laminar Propane-Air Flame in a Weak Electric Field," *Combustion, Explosion, and Shock Waves*, vol. 48, no. 2, pp. 130-135, 2012.

[25] Schmidt, J.B. and Ganguly, B.N., "Effect of Pulsed, Sub-Breakdown Applied Electric Field on Propane/Air Flame through Simultaneous OH/Acetone PLIF," *Combustion and Flame*, vol. 160, no. 12, pp. 2820-2826, 2013.

[26] Yagodnikov, D.A., "Effect of an Electric Field on the Stabilization of a Turbulent Propane-Air Flame," *Combustion, Explosion, and Shock Waves*, vol. 34, no. 1, pp. 16-19, 1998.

[27] Kim, M.K., Ryu, S.K., Won, S.H. and Chung, S.H., "Electric Fields Effect on Liftoff and Blowout of Nonpremixed Laminar Jet Flames in Coflow," *Combustion and Flame*, vol. 157, no. 1, pp. 17-24, 2010.

[28] Garanin, A.F., Tret'yakov, P.K. and Tupikin, A.V., "Effect of Constant and Pulsed-Periodic Electric Fields on Combustion of a Propane-Air Mixture," *Combustion, Explosion, and Shock Waves*, vol. 44, no. 1, pp. 18-21, 2008.

[29] Fialkov, A.B., "Investigation on Ions in Flames," *Progress in Energy and Combustion Science*, vol. 23, no. 5-6, pp. 399-528, 1997.

[30] Pitts, W.M., "Assessment of Theories for the Behavior and Blowout of Lifted Turbulent Jet Diffusion Flames," *Symposium (International) on Combustion*, vol. 22, no. 1, pp. 427-509, 1988.

[31] Peters, N.H. and Williams, F.A., "Liftoff Characteristics of Turbulent Jet Diffusion Flames," *AIAA Journal*, vol. 21, no. 3, pp. 423-429, 1983.

[32] Kalghatgi, G.T., "Lift-off Heights and Visible Lengths of Vertical Turbulent Jet Diffusion Flames in Still Air," *Combustion Science and Technology*, vol. 41, no. 1-2, pp. 17-29, 1984.

[33] Vanquickenborne, L. and Tiggelen, A.V., "The Stabilization Mechanism of Lifted Diffusion Flames," *Combustion and Flame*, vol. 10, no. 1, pp. 59-69, 1966.

[34] Buckmaster, J.D., "Edge-Flames," *Progress in Energy and Combustion Science*, vol. 28, no. 5 pp. 435-475, 2002.

[35] Broadwell, J.E., Dahm, W.J.A. and Mungal M.G., "Blowout of Turbulent Diffusion Flames," *Symposium (International) on Combustion*, vol. 20, no. 1, pp. 303-310, 1984.

[36] Wu, C.Y., Chao, Y.C., Cheng, T.S., Li, Y.H., Lee, K.Y. and Yuan, T., "The Blowout Mechanism of Turbulent Jet Diffusion Flames," *Combustion and Flame*, vol. 145, no. 3**,** pp. 481-494, 2006.

[37] Tummers, M.J., Hubner, A.W., Veen van, E.H., Hanjalic, K. and van der Meer, T.H., "Hysteresis and Transition in Swirling Nonpremixed Flames," *Combustion and Flame*, vol. 156, no. 2, pp. 447-459, 2009.

[38] Papanikolaou, N, and Wierzba, I., "Effect of Burner Geometry on the Blowout Limits of Jet Diffusion Flames in a Co-flowing Oxidizing Stream," *ASME Journal of Energy Resources Technology*, vol. 118, no. 2**,** pp. 134-139, 1996.

[39] Hutchins, A.R., Kribs, J.D., Muncey, R.D. and Lyons, K.M., "Assessment of Stabilization Mechanisms of Confined, Turbulent, Lifted Jet Flames: Effects of Ambient Coflow," *2013 ASME Power Conference Proceedings*, Boston, MA, 2013.

[40] Hutchins, A.R., Kribs, J.D., Muncey, R.D., Reach, W.A. and Lyons, K.M., "Experimental Observations of Nitrogen Diluted Ethylene and Methane Jet Flames," *2013 ASME Summer Heat Transfer Conference Proceedings*, Minneapolis, MN, 2013.

[41] Kribs, J.D., Moore, N.J., Hasan, T.S. and Lyons, K.M., "Nitrogen-Diluted Methane Flames in the Near- and Far-Field," *ASME Journal of Energy Resources Technology*, vol. 135, no. 4, pp. 1-10, 2013.

[42] Donnerhack, S. and Peters, N.H., "Stabilization Heights in Lifted Methane-Air Jet Diffusion Flames Diluted with Nitrogen," *Combustion Science and Technology*, vol. 41, no. 1-2, pp. 101-108, 1984.

[43] Wilson, D.A. and Lyons, K.M., "On Diluted-Fuel Combustion Issues in Burning Biogas Surrogates," *ASME Journal of Energy Resources Technology*, vol. 131, no. 4, pp. 1-9, 2009.

[44] Papanikolaou, N. and Wierzba, "The Effects of Burner Geometry and Fuel Composition on the Stability of a Jet Diffusion Flame," *ASME Journal of Energy Resources Technology*, vol. 119, no. 4, pp. 265-270, 1997.

[45] Schefer, R.W., "Hydrogen Enrichment for Improved Lean Flame Stability," *International Journal of Hydrogen Energy*, vol. 28, no. 10, pp. 1131-1141, 2003.

[46] Kribs, J.D., Hutchins, A.R., Reach, W.A., Hasan, T.S. and Lyons, K.M., "Effects of Hydrogen Enrichment of the Reattachment and Hysteresis of Lifted Methane Flames," *2013 ASME Power Conference Proceedings*, Boston, MA, 2013.

[47] Bak, M.S., Im, S.K., Mungal, M.G. and Cappelli, M.A., "Studies on the Stability Limit Extension of Premixed and Jet Diffusion Flames of Methane, Ethane, and Propane Using Nanosecond Repetitive Pulsed Discharge Plasmas," *Combustion and Flame*, vol. 160, no. 11, pp. 2396-2403, 2013.

[48] Kumar, S., Paul, P.J. and Mukunda, H.S., "Prediction of Flame Liftoff Height of Diffusion/Partially Premixed Jet Flames and Modeling of Mild Combustion Burners," *Combustion Science and Technology*, vol. 179, no. 10, pp. 2219-2253, 2007.

[49] Ogami, Y. and Kobayashi H., "Laminar Burning Velocity of Stoichiometric CH_4/Air Premixed Flames at High-Pressure and High-Temperature," *JSME International Journal*, vol. 48, no. 3, pp. 603-609, 2005.

[50] Thring, M.W. and Newby, M.P., "Combustion Length of Enclosed Turbulent Jet Flames," *Symposium (International) on Combustion*, vol. 4, no. 1, pp. 789-796, 1953.

[51] Guruz, A.G., Guruz, H.K., Osuwan, S. and Steward, F.R., "Aerodynamics of a Confined Burning Jet," *Combustion Science and Technology*, vol. 9, no. 3-4, pp. 103-110, 1974.

[52] Yumlu, V.S., "The Effects of Additives on the Burning Velocities of Flames and their Possible Prediction by a Mixing Rule," *Combustion and Flame*, vol. 12, no. 1, pp. 14-18, 1968.

[53] Brown, C.D., Watson, K.A. and Lyon, K.M., "Studies on Lifted Jet Flames in Coflow: The Stabilization Mechanism in the Near- and Far-Fields," *Flow, Turbulence and Combustion*, vol. 62, no. 3, pp. 249-273, 1999.

[54] Tieszan, S.R., Stamps, D.W. and O'Hern, T.J., "A Heuristic Model of Turbulent Mixing Applied to Blowout of Turbulent Jet Diffusion Flames," *Combustion and Flame*, vol. 106, no. 4, pp. 463-466, 1996.

[55] Weinberg, F.J. and Carleton, F.B., "Electric Field-Induced Flame Convection in the Absence of Gravity," *Nature*, vol. 330, pp. 635-636, 1987.

[56] Rickard, M., Dunn-Rankin, D., Weinberg, F.J. and Carleton, F.B., "Characterization of Ionic Wind Velocity," *Journal of Electrostatics*, vol. 63, no. 6-10, pp. 711-716, 2005.

[57] Robinson, M., "Movement of Air in the Electric Wind of the Corona Discharge," *Transactions of the American Institute of Electrical Engineers, Part I: Communication and Electronics*, vol. 80, no. 2, pp. 143-150, 1961.

[58] Nayagam, V., Balasubramaniam, R. and Ronney, P.D., "Diffusion Flame-Holes," *Combustion Theory Modelling*, vol. 3, pp. 727-742, 1999.

[59] Rajaratnam, N., "Turbulent Jets," Elsevier, New York, N.Y., 1976.